Energy Advances

ROYAL SOCIETY OF CHEMISTRY

REVIEW ARTICLE

View Article Online
View Journal | View Issue

Cite this: *Energy Adv.*, 2023, **2**, 1263

Recent technological advances in designing electrodes and electrolytes for efficient zinc ion hybrid supercapacitors

Himanshu Gupta,[a] Manoj Kumar,[a] Debasish Sarkar *[a] and Prashanth W. Menezes *[bc]

Rechargeable zinc ion hybrid supercapacitors (ZIHSCs) have gained significant research and technological interest because they synergize the benefits of zinc ion batteries (ZIBs) with high energy density and supercapacitors (SCs) with high power density and cycling stability. They are considered as promising candidates for next-generation high-performance energy storage systems (ESSs) owing to their satisfactory energy-power combination, inherent safety features, low cost, and excellent electrochemical stability. The power of ZIHSCs lies in their suitably chosen electrode (cathode and anode) materials, optimized electrode architecture, and optimized electrolyte governing charge storage behavior. Although ZIHSCs have made some remarkable advancements in this regard, the current scenario is distant from what is necessary for their widespread practical application and hence, poses a major scientific as well as technological challenge to the research community. Therefore, further development in understanding of the intricate Zn ion storage mechanism in rationally designed novel electrode materials is highly coveted towards realizing novel, multi-functional ZIHSC devices with exceptional energy-power densities and ultra-long cycle life. This review is designed to cover the foundations and current scientific and technological achievements in the field of ZIHSCs, including their compositions, types, electrode materials, electrode design strategies, charge storage mechanisms, beneficial traits, electrolyte compositions, and newly created devices. Additionally, potential drawbacks with current generation ZIHSCs with possible solution strategies are also highlighted. The goal of this in-depth analysis is to provide a useful understanding of ZIHSCs that would be effective for their large-scale development and practical deployment as high-performance ESSs in a variety of applications.

Received 7th June 2023,
Accepted 13th July 2023

DOI: 10.1039/d3ya00259d

rsc.li/energy-advances

1. Introduction

Green energy is one of the most important topics in the 21st century. With the fast depletion of fossil fuels and progressively worsened environmental pollution due to exorbitant fossil-fuel consumption, there is a high demand for renewable and clean energy sources that can substitute fossil fuels and augment the efficient use of green energy, and enable the sustainable development of our economy and society.[1,2] However, to tackle the challenge of intermittency issues with renewable energy resources, the need for energy storage becomes inevitable for the use of green energy whenever in need. Hence, energy storage, an intermediate step to versatile, clean, and efficient energy use, has received worldwide attention and increasing research interest.[3]

Currently, batteries and supercapacitors are the two leading electrochemical energy-storage systems (ESSs) among the various energy-storage devices. Lithium-ion batteries (LIBs) have found enormous applications primarily in consumer electronics and to some extent in electric traction owing to their high energy density (up to $\sim$300 W h kg^{-1}).[4,5] However, their utility is still limited by several factors, including limited availability of Li-metal, its highly reactive nature causing severe safety concerns, resistive losses due to slow electron and ion transport, as well as dendrite development and heat buildup when these batteries are used at high current rates, and short lifetime.[6,7] In this regard, high power density, fast charge–discharge traits, and remarkable cycle life (>100 000 cycles) of electrochemical capacitors (also known as supercapacitors,

[a] *Department of Physics, Malaviya National Institute of Technology Jaipur, Rajasthan-302017, India. E-mail: deb.sarkar1985@gmail.com, debasish.phy@mnit.ac.in*
[b] *Material Chemistry Group for Thin Film Catalysis-CatLab, Helmholtz-Zentrum Berlin für Materialien und Energie, Albert-Einstein-Str. 15, 12489 Berlin, Germany. E-mail: prashanth.menezes@helmholtz-berlin.de*
[c] *Department of Chemistry, Technical University of Berlin, Straße des 17 Juni 135. Sekr. C2, 10623, Berlin, Germany. E-mail: prashanth.menezes@mailbox.tu-berlin.de*

SCs) make them a viable alternative to batteries in many situations. Consequently, SCs have sparked a growing interest in applications requiring rapid charging, outstanding cycle life, and high power density.[8–12] However, the relatively low energy densities (5–10 W h kg^{-1}) of SCs have severely limited their field of applications. Therefore, the development of SCs with high energy-power densities and long cycle life is highly coveted for the effective utilization of renewable energy. A hybrid supercapacitor (HSC) consisting of battery-type and capacitor-type electrodes could combine these advantages of batteries and supercapacitors (SCs) and attain high energy density without sacrificing high power density and extraordinary cycle life traits.[13,14] For instance, Li-ion-based hybrid SCs (LISCs) have been one of the competent energy storage choices in recent years owing to their energy and power densities in excess of 200 W h kg^{-1} and 10 kW kg^{-1}, respectively. Future practical uses of LISCs, however, look challenging because of the limited availability and inflammable character of lithium. In order to address the

Himanshu Gupta

Himanshu Gupta received his master's degree in Physics from Malaviya National Institute of Technology Jaipur, Rajasthan, India, in the year 2020. He is currently pursuing his PhD under the supervision of Dr Debasish Sarkar in the Department of Physics at Malaviya National Institute of Technology Jaipur, Rajasthan, India. His work is mainly focused on the synthesis and characterization of nanomaterials for energy harvesting and storage applications, with a particular emphasis on the investigation of innovative nanostructured electrode materials for high-voltage metal-ion hybrid supercapacitors. He is also interested in biomass-derived carbon materials for the purpose of electrochemical energy storage.

Manoj Kumar

Manoj Kumar is currently working as an Assistant Professor in the Department of Physics, Malaviya National Institute of Technology Jaipur, India. He completed his PhD in Physics from the University of Rajasthan, Jaipur, India. During his PhD studies, he also worked at Max Planck Institute for Chemical Physics of Solids, Dresden, Germany, from 2007–2009. He worked as a postdoctoral researcher at the Institute of Solid-State Physics, IFW Dresden, Germany, during 2010–2011 and at the Faculty of Engineering, NUS, Singapore, during 2012–2014. His core area of research includes nanocomposites, nanomaterials, CNTs and their devices, thermoelectric power generators, electronic and magnetic phase transitions in perovskite oxides, Fe-based superconductors, topological insulators, and 2DEG materials at high pressures, low temperatures, and high magnetic fields, as well as the synthesis and characterization of nano-crystalline, thin films, and bulk single crystals through different routes.

Debasish Sarkar

Debasish Sarkar received his PhD degree from S N Bose National Centre for Basic Sciences, India, in the year 2014. He carried out his post-doctoral research work as an INSPIRE Faculty Fellow at Indian Institute of Science, India, and as a Research Associate at Clarkson University, New York, USA. Currently, he is serving as an Assistant Professor in the Department of Physics at Malaviya National Institute of Technology Jaipur, India. His research activities are focused on the development of novel nanostructured electrode materials for electrochemical energy (H_2) generation through water splitting, and energy storage through metal-ion batteries and supercapacitors.

Prashanth W. Menezes

Prashanth W. Menezes is a head of materials chemistry for the thin film catalysis group at CatLab of Helmholtz-Zentrum Berlin für Materialien und Energie and the inorganic materials group at Technische Universität Berlin. He received his PhD from Max Planck Institute for Chemical Physics of Solids in Dresden, following which he moved to Technische Universität München and then to Technische Universität Berlin to work on energy catalysis. His research focuses on the design, development, and structural understanding of novel unconventional catalysts in heterogeneous catalysis, especially in the area of redox oxygen catalysis, (photo)electrocatalytic water splitting and electrochemical redox reactions.

aforementioned issues, other systems based on monovalent or multivalent cations, such as sodium (Na^+), potassium (K^+), magnesium (Mg^{2+}), zinc (Zn^{2+}), calcium (Ca^{2+}), and aluminum (Al^{3+}) have been explored rationally.[14–16] However, they are also not without their shortcomings! Several intrinsic flaws, including safety hazards caused by the reactive metallic Na/K and the inflammable nature of organic electrolytes, have somewhat restricted their widespread usage in the ESS and electronics industry.[15,16] Meanwhile, multivalent cations, including Ca^{2+}, Mg^{2+}, Zn^{2+}, and Al^{3+}, have demonstrated some advantageous traits like fast charge transfer dynamics as compared to the monovalent cations.[17–19] Benefitting from the suitable redox potential of −0.76 V *vs.* standard hydrogen electrode (SHE) and a satisfying theoretical capacity of 820 mA h g^{-1} (equivalent to 5855 mA h cm^{-3}) of the Zn electrode, Zn ion-based HSC devices have garnered a lot of attention as potential alternative ESSs after carefully examining their dynamics, performance, and security.[20,21]

Zinc ion hybrid supercapacitors (ZIHSCs) are composed of battery-type and capacitor-type electrodes with Zn-containing electrolytes. In ZIHSCs, energy is stored through reversible ion adsorption/desorption on the capacitor-type electrode, while Zn-ion plating/stripping processes occur at the battery-type electrode. As these two electrodes operate in different potential windows, the ZIHSCs could offer a wide potential window and consequently, a high energy density too. As illustrated in Fig. 1, the energy density and the power density of ZIHSCs are highly competitive in contrast with other standard ESSs. Furthermore, the materials used for both electrodes are highly stable (in a neutral/mild neutral electrolyte system), ensuring ultralong cycling stability. Therefore, ZIHSCs have great potential to be next-generation ESSs with satisfactory energy and power densities, and excellent cycling stability.[22]

After Wang *et al.* published the first report on ZIHSC in 2016, the technology has developed since then and has become the cutting edge of energy storage research worldwide.[23] However, a thorough and systematic summary of current technical advancements in ZIHSCs, covering their fundamentals, novel electrode materials, innovative development strategies, and device design and manufacturing, is highly coveted considering the tremendous potential as future ESSs.[24] Keeping this in mind, this study begins by outlining the fundamentals of ZIHSCs, including their configurations, operating principles, categories, and associated difficulties in achieving optimized performance. Then, we discuss the synthesis approach (especially the solution method and pyrolysis method) of electrode materials (including capacitors and battery-type materials) and their recent developments, various electrolytes (such as aqueous, non-aqueous, and new types of electrolytes), and novel device designs (such as flexible, micro, and photo-rechargeable devices, *etc.*). Recent advancements in electrode materials for ZIHSCs primarily include advanced nanostructures of carbon (such as activated carbon [AC], porous carbon [PC], heteroatom doped carbons [HADCs], *etc.*), metal oxides, metal carbides (MXenes), metalorganic frameworks (MOFs), and conducting polymers, *etc.* In conclusion, an overview of the current *status quo* is provided, along with useful perspectives for developing cutting-edge ZIHSCs. This review article is anticipated to provide an understanding of workable techniques for high-performance ZIHSCs and help to further scientific advancements in electrode and electrolyte technologies for ZIHSC devices.

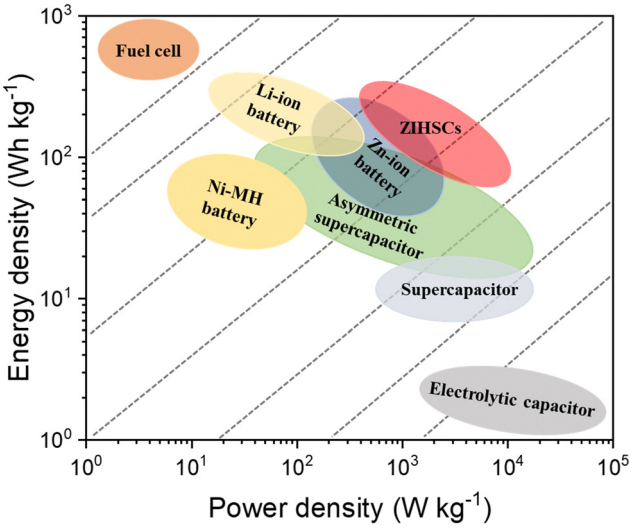

Fig. 1 Ragone plot of Zn-ion hybrid supercapacitors (ZIHSCs) comparing their performance with other standard energy storage systems (ESSs).

2. Fundamentals of ZIHSCs

2.1 Cell configuration and types

As shown in Fig. 2, the primary components of a ZIHSC are the capacitor- and battery-type electrodes, the electrolyte, and the separator. Electrode materials are an essential part of ZIHSCs and significantly impact the performance of ZIHSCs. Most research on capacitive-type electrode materials in ZIHSCs focuses on carbon-based or pseudocapacitive materials, while metallic Zn and metal-based oxides are extensively researched for their use as battery-type electrodes. There are two distinct categories of ZIHSCs, delineated by the electrode materials that have been used:

(I). Type I: the cathode is made of carbon or pseudocapacitive materials and the anode is made of Zn metal or modified Zn metal. Here, on the capacitor side, the charge is stored through adsorption/desorption or intercalation/deintercalation of electrolytic ions, while the Zn plating/stripping mechanism transpires on the battery-side electrode.

(II). Type II: the anode might be made of carbon or a pseudocapacitive substance, whereas the cathode is made of metal oxides and sulfides used in batteries. The charge storage mechanism is adsorption/desorption or intercalation/deintercalation type on the anodic side; however, on the cathodic side, insertion/de-insertion of Zn^{2+} ions in and out of the electrode governs its capacity.

Both types have their own advantages; high power density and long cycle life are features of the former, while high energy

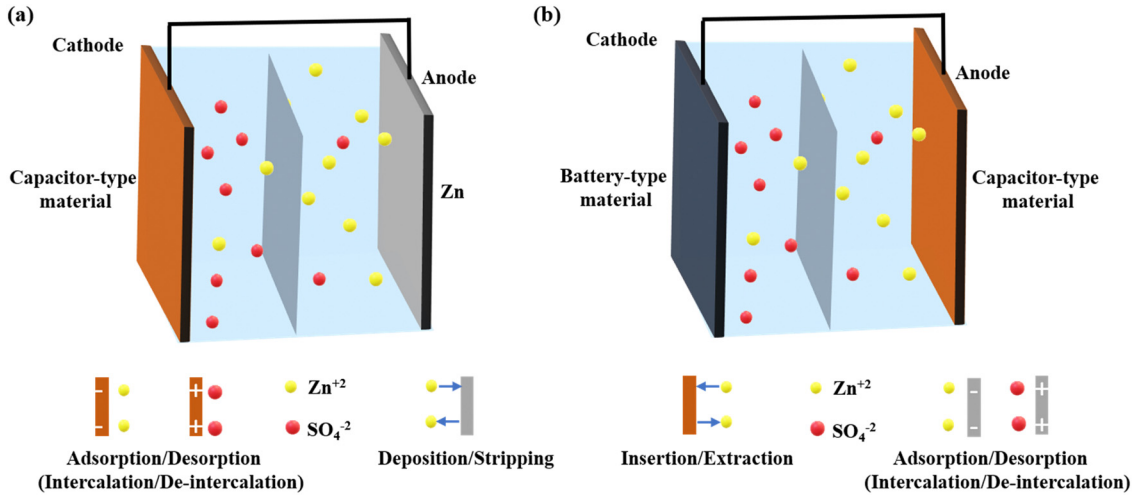

Fig. 2 Schematic illustration of the cell configuration and the working principle of (a) the first type of ZIHSC and (b) the second type of ZIHSC.

density is unique to the latter. Therefore, ZIHSCs are a hybrid of the two distinct electrode materials where a synergistic combination of significantly different charge storage mechanisms and dynamics offer superior cycling stability, power density, and energy storage.

2.2 Working mechanism

Usually, it is believed that capacitor-type electrodes store energy through ions' adsorption as well as intercalation and release *via* the process of desorption as well as de-intercalation. In battery-type electrodes, energy is stored through ions' deposition or insertion and released through ions' stripping or extraction. The working mechanism of the first type of ZIHSCs is shown in Fig. 2a. During the charging process, negative ions (anions) move from the electrolyte and form an electric double layer (EDL) (or undergo faradaic intercalation) by adsorption onto (or intercalation into) the cathode surface. Simultaneously, positive ions (Zn^{2+}) are deposited onto the Zn anode from the electrolyte, as shown in eqn (1). In contrast to the charging process, the discharge process involves the diffusion of anions and cations back into the electrolyte from respective electrodes. Superior energy and power densities of the ZIHSCs are possible because of the reversible ion flow between the electrolyte and the electrode.[18,24]

The charge storage mechanism in carbon electrodes is still a topic of debate. Many researchers have hypothesized that anions are crucial as leading carriers, migrating to and adsorbing on the carbon electrode to produce an EDL during charging before diffusing back into the electrolyte during the discharge process, as represented by eqn (2). Others, however, argue that the capacity was considerably enhanced by the adsorption/desorption of Zn^{2+} cations on the carbon surface (eqn (3)). Kang and co-authors noted that SO_4^{2-} anions adsorbed on or desorbed from the carbon surface when the operating potential was higher than zero-charge potential, but electrostatic adsorption/desorption of cations dominated when the potential was lower than the zero-charge potential.[19] Therefore, they argued that the dominant adsorption/desorption of ions is determined by the operating potential and zero-charge potential of carbon materials. Furthermore, when using heteroatom-doped carbon materials, chemical adsorption/desorption of cations may also occur because heteroatoms are demonstrated to contribute additional pseudocapacitance to the total capacity. Eqn (4) and (5) describe the chemical adsorption and desorption processes on different heteroatoms (N, O) generally found or introduced in carbons for bettered capacity. In addition, several investigations have also shown that the carbon cathode undergoes irreversible side reactions (as represented by eqn (6)–(8)) and forms zinc hydroxide sulfate hydrate ($Zn_4SO_4(OH)_6{\cdot}xH_2O$). The pH shift on the carbon electrode's surface may be responsible for the creation of $Zn_4SO_4(OH)_6{\cdot}xH_2O$, which further indicates the involvement of H^+ or OH^- ions in the process.[25–27]

Zn anode:

$$Zn^{2+} + 2e^- \leftrightarrow Zn \quad (1)$$

Carbon-based cathode:

(1) Physical adsorption/desorption process

$$C + X^- \leftrightarrow C\|X^- \quad (2)$$

$$C + Zn^{2+} \leftrightarrow C\|Zn^{2+} \quad (3)$$

where C represents the carbon material and X^- represents the anion in the electrolyte.

(2) Chemical adsorption/desorption process

$$C\cdots O + Zn^{2+}/H^+ + e^- \leftrightarrow C\cdots O\cdots Zn/C\cdots O\cdots H \quad (4)$$

$$N\cdots O + Zn^{2+}/H^+ + e^- \leftrightarrow N\cdots O\cdots Zn/C\cdots O\cdots H \quad (5)$$

where $C\cdots O$ and $N\cdots O$ represent the functional groups on carbons.

(3) Precipitation/dissolution process

$$6H_2O \leftrightarrow 6OH^- + 6H^+ \quad (6)$$

$$4Zn^{2+} + 6OH^- + SO_4^{2-} + xH_2O \leftrightarrow Zn_4SO_4(OH)_6{\cdot}xH_2O \quad (7)$$

$$Zn_4SO_4(OH)_6{\cdot}xH_2O \leftrightarrow 4Zn^{2+} + SO_4{}^{2-} + xH_2O \quad (8)$$

In Fig. 2b, we have demonstrated the inner workings of the second category of ZIHSCs. Basically, this type of ZIHSC consists of a battery-type cathode and a capacitor-type anode with a zinc salt-based electrolyte. In contrast to the first type of ZIHSC, this device avoids using unstable Zn-foil, which is advantageous for improving the overall specific capacity and performance of the ZIHSC. An important difference between these two types is that the latter provides a wider working voltage window, which subsequently increases the energy density of the device. The basic charge storage mechanism of this type of ZIHSC is thought to be based on Zn^{2+} ion insertion/extraction onto the cathode's surface and adsorption/desorption or intercalation/de-intercalation of ions onto the surface of the carbon anode. Generally, the discharging process causes the transportation of Zn^{2+} ions from the electrolyte and diffusion into the cathode, whereas the adsorption or intercalation of anions occurs in the carbon anode. On the other hand, Zn^{2+} ions are transferred from the cathode to the electrolyte, and adsorbed (or intercalated) anions are desorbed into (or de-intercalate into) the electrolyte during the charging process.[24,28]

2.3 Merits and challenges with ZIHSCs

Merits

Superior capacity and power output. For ZIHSCs, the capacitor-type electrode offers large power output through fast ion adsorption/desorption (or intercalation/de-intercalation) reactions, whereas the battery-type anode (or cathode) provides a large capacity through the zinc ions deposition/stripping (or insertion/extraction) reactions. Therefore, ZIHSCs offer higher capacity than electric double layer capacitors (EDLCs) and a superior power density than ZIBs, benefiting from diverse charge storage mechanisms of battery-type and capacitor-type electrodes.

Relatively wide working potential window. It is well accepted that the electrode materials and electrolytes affect the working voltage of EDLCs. In aqueous electrolytes, the working potential window of ZIHSCs could reach well over 1.5 V (much larger than EDLCs with a voltage window limited to $\sim$1 V), owing to the synergistic operation of two different electrodes in two different potential ranges.[24]

High level of safety. Aqueous ZIHSCs are substantially safer as compared to non-aqueous ZIBs and EDLCs owing to the concealed hazard caused by the use of non-aqueous inflammable electrolytes.

Material abundance. Due to the natural abundance of Zn, ZIHSC devices are more likely to be used in large-scale, real-world commercial applications.

Challenges. Besides having several technological advantages over traditional EDLCs and Zn-ion batteries, including high energy/power output, relatively higher working potential, high safety, and material's abundance, ZIHSCs are also plagued with several disadvantages like poor cycle life and rate capability caused by imbalanced electrode kinetics. The basic electrochemistry involved in ZIHSCs is highly complex owing to multiple electrochemical processes occurring simultaneously, making it difficult to grasp the underlying mechanisms. Some debate exists in the present scientific literature verifying energy storage technologies and determining the identity of the resulting intermediates. More work and analyses are urgently required to identify and analyze the potential by-products of charge storage processes. The real-time detection of intermediates and a thorough understanding of electrochemical behaviors will get benefitted significantly from the advancement of *in situ* or operando instruments and techniques (such as *in situ* X-ray powder diffraction, *in situ* Raman spectroscopy, *in situ* X-ray absorption spectroscopy, *etc.*).[20] Moreover, in order to realize practical ZIHSCs with satisfactory performance, several obstacles must be overcome as demonstrated in Fig. 3. The primary difficulties with current generation ZIHSCs are their low energy density and poor cycling performance of the Zn anode. Energy density is directly proportional to the capacitance and the square of the potential window. So, increasing the potential window is beneficial for improving energy density besides increasing capacitance. Now, capacitance is directly related to the specific surface area (SSA) that the electrode materials are providing for reversible adsorption/desorption of Zn^{2+} ions together with abundant pore accessibility for faster ion movements. Although the ionic size of Zn^{2+} is close to Li^+, its diffusivity and solid-state solubility in the bulk of the electrode material are restricted by its large atomic mass and high positive polarity. Therefore, significant research works are currently ongoing toward the development of high surface area porous materials for realizing both cathodes and anodes in ZIHSCs. Abundant pores with micro to mesoporous size range could positively affect the Zn^{2+} ion diffusion rate during charge/discharge processes and hence improve the rate performance too. Furthermore, a potential window is primarily driven by the electrochemical stability of electrolytes used in an electrochemical cell. In neutral and mild acidic electrolytes, parasitic reactions, such as the HER, OER, and oxidization of porous carbon cathodes limit the potential window. Zinc hydroxide is found to form when Zn metal reacts with hydroxide ions in alkaline electrolytes, which may lower the electrolyte's conductivity and make Zn anodes more polarised.

Due to the dendrite development, the HER, and corrosion reactions, the Zn anode shows limited cycle life compared to carbon cathodes. Zn dendrite formation is a complex process originating from the uneven ion distribution and electric field on the anode plate. Dendrites increase the specific surface area (SSA) of the Zn anode during the charge/discharge processes and accelerate the HER rate. The HER consumes protons (H^+) in aqueous electrolytes and forms hydroxide (OH^-) ions. The Zn anode interacts with these ions and accumulates zinc hydroxide species on the surface of the zinc anode, resulting in dendrite formation.[23] This has caused limited service life of ZIHSCs, which is far below commercial EDLCs with life well above 100 000 cycles. Recent developments in electrolytes with suitable anions like $CF_3SO_3{}^-$ could inhibit the formation of

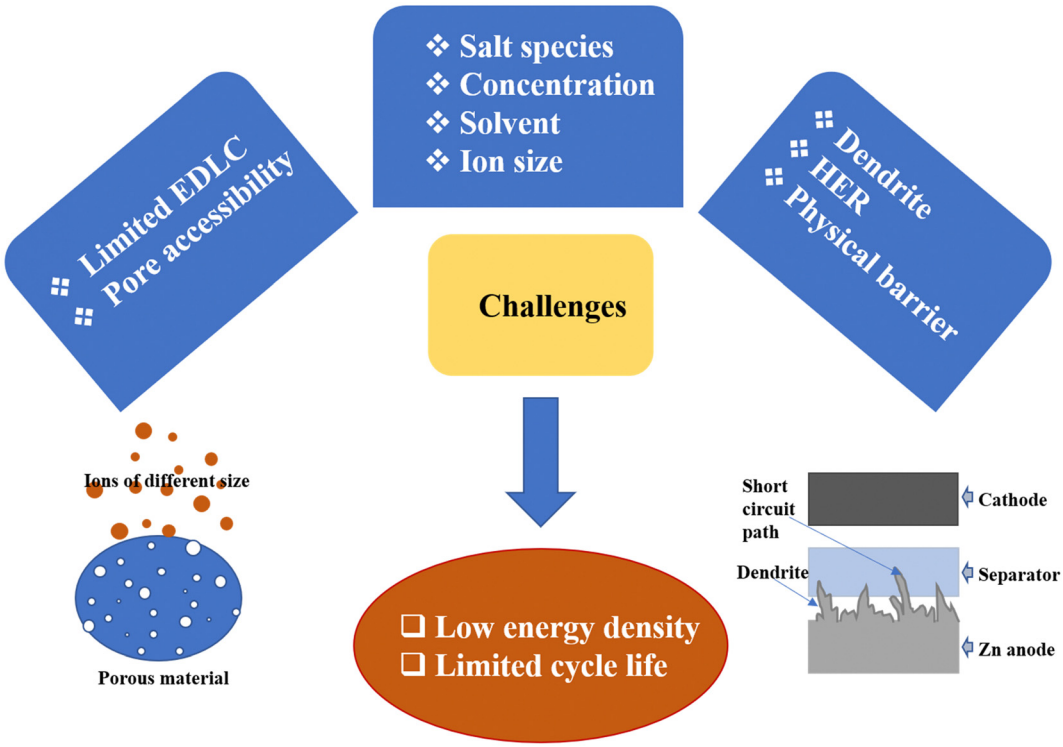

Fig. 3 A summary of the challenges prevailing with current generation ZIHSCs which need to overcome to realize high-performance ZIHSCs.

byproducts and improve the Zn^{2+} plating/stripping efficiency to eliminate capacity-killing dendrite formation.

Another major concern with ZIHSCs is the kinetic imbalance between capacitor-type and battery-type electrodes causing poor rate capability for the device. It is quite understandable that a charge storage process governed by bulk diffusion of ions in and out of battery-type electrodes would not match the fast rate of ion adsorption/desorption on the capacitor-type electrodes, preventing ZIHSCs from achieving high energy density at high power densities. Researchers have come up with several innovative ideas like modification of the surface and structure of the Zn electrode, and designing nanostructured electrode surfaces to accelerate the ion insertion/de-insertion rates to and from the electrode material, thus matching with the fast charge storage kinetics of capacitor-type electrodes, and resulting in extraordinary energy and power combinations for ZIHSCs.

3. Synthesis approaches of electrode materials for ZIHSCs

3.1 Solution method

3.1.1 Room temperature reaction. Room temperature reaction is the simplistic, most straightforward, and widely accepted method in which the precursors of different materials are taken into reaction, and the desired material or structure is prepared. Most of the MOF-derived materials and their doping with heteroatoms are carried out by this method. For instance, Yang *et al.* prepared ZIF-8 dodecahedra by this method.[29] In detail, 3.12 g 2-methylimidazole was dissolved into 200 mL of methanol solution with 1.05 g $C_4H_6O_4Zn{\cdot}2H_2O$ and 3.2 g polyvinylpyrrolidone (PVP). Then, the prepared solution was stirred vigorously for 1 h and subsequently aged at room temperature for 24 h. Following centrifugation, methanol washing, and overnight drying at 60 °C, the white ZIF-8 precipitates were collected. As confirmed by the SEM and TEM analysis, the resultant material has a polyhedral shape with an almost uniform size distribution.

3.1.2 Hydrothermal method. A hydrothermal method is essential for preparing MOF precursors, different metal oxides, *etc.*, and refers to preparing materials by dissolving precursors in water solvent in an autoclave followed by recrystallization of the desired materials at elevated temperatures. It is a low-cost, one-pot, eco-friendly, and efficient solution method for preparing unique morphologies of electrode materials. Hence, it has found a wide range of applications in the synthesis of hybrid materials owing to the high reactivity, controllability, and unique condensed phase of reactants. Chemical and physical transformation of novel materials can be achieved under high temperature and high-pressure liquid conditions.[30] Li *et al.* synthesized a Co_9S_8@MnO_2 core–shell heterostructure.[31] Firstly, they dissolved 0.1422 g $KMnO_4$ in 30 mL of DI water and stirred it with a magnetic stirrer for 30 min. Then, they used a piece of prefabricated Co_9S_8/CC (CC stands for carbon cloth) as a substrate and dipped it into the prepared solution, and transferred the same into an autoclave. The hydrothermal reaction was carried out at 140 °C for 2 h to obtain the Co_9S_8@MnO_2/CC heterostructure.

Using a standard, one-step hydrothermal process, Zhao *et al.* synthesized N/P co-doped graphene (NPG) by dissolving 120 mg of GO powder in 40 mL of DI and sonicating the mixture for 1 hour to get a 3 mg mL^{-1} GO dispersion.[32] Next, 3 mL of phytic acid (PA) and 3 mL of ethylenediamine (EDA) were added to the GO dispersion, and the mixture was agitated at room temperature for 2 hours to incorporate the phosphorus and nitrogen. The above solution was transferred to a high-pressure reactor and hydrothermally reacted at 180 °C for 12 h, followed by natural cooling to obtain a cylindrical form of the NPG hydrogel. Ren *et al.* synthesized hybrid cathode material Zn_xMnO_2-CNTs.[33] In detail, 0.024 mol $KMnO_4$ and 0.024 mol $Zn(NO_3)_2{\cdot}6H_2O$ were dissolved in 75 mL of deionized water followed by dropwise addition of 2 mL of H_2SO_4 (98%) at room temperature under continuous stirring. The solution was then placed in an autoclave, sealed, and heated at 140 °C for 3.5 h. The resultant brown precipitate of Zn_xMnO_2 nanowires was washed several times with DI and freeze-dried for 24 h. Similarly, Liang *et al.* synthesized lamellar vanadium oxide as a cathode material.[34] 0.3 g V_2O_5 and 5 mL H_2O_2 were dispersed in 30 mL deionized water and stirred at 40 °C for 30 min. Then, 96 mg Ni $(NO_3)_2{\cdot}6H_2O$ was added and stirred for another 30 min to obtain a clear and transparent solution, which was transferred into a Teflon-lined autoclave and kept at 180 °C for 48 h. The precipitate was washed and dried at 60 °C overnight to get the final product. Similarly, He *et al.* prepared δ-MnO_2 and Zn-MnO_2 by a hydrothermal method for their use as electrodes in ZIHSCs.[35]

3.1.3 Solvothermal method. Similar to the hydrothermal method, the solvothermal method uses a non-aqueous solution rather than an aqueous one. As opposed to the aqueous medium, organic solvents are investigated as reaction media throughout a wide temperature range, preventing agglomeration and controlling the reaction products' shape and phase structure. Nanostructured materials' morphological differences decrease ion diffusion lengths, which facilitates easy electrolyte ion and electron migration and hence improves electrochemical performance. Solvents may create a variety of complexes with the ions, which might change the nucleation and development process.[5,36] For instance, Jiang *et al.* prepared a fluffy graphene hydrogel (FGH) architecture and coupled it with high capacity redox-active phenanthraquinone (PQ).[37] The PQ-FGH composite electrode ensures rapid electron transfer between PQ and the graphene sheets as well as fast ion transportation during electrochemical reactions. Similarly, Xu. *et al.* prepared a *p*-phenylenediamine (PPD) functionalized reduced graphene oxide (RGO) film to utilize as a positive electrode in ZIHSCs with a Zn foil negative electrode.[38] In detail, first PPD was dissolved in water and mixed with GO aqueous solution under stirring to obtain a uniform RGO-PPD dispersion solution. Then, the mixed solution was evaporated at 70 °C to form a RGO-PPD hybrid composite film, and then the prepared film was cut into a quadrate of 1×1 cm^2. Finally, the RGO-PPD film was further reduced by solvothermal reaction in the PPD/ethanol solution. Similarly, Wei *et al.* synthesized MOF ZIF-8 by a solvothermal method taking zinc nitrate hexahydrate, 2-methylimidazole, and *N*,*N*-dimethylformamide as starting precursors.[39] Furthermore, Xiong *et al.* synthesized $Ni_3(OH)_2$-$(C_8H_4O_4)_2(H_2O)_4$ MOF by a one-pot solvothermal method using nickel nitrate hexahydrate, terephthalic acid, and N,N-dimethylformamide as precursors.[40]

3.1.4 Electrochemical deposition. Electrochemical deposition is a versatile technique by which a thin desired metallic coating can be obtained onto the surface of another metal/substrate by simple electrolysis of an aqueous solution containing the desired metal ion or its complex.[41] In this method, metal ions become solid metal and deposit on the electrode surface if sufficient electric current passes through the electrolyte solution. For instance, Wu *et al.* prepared a 3D stacked lamellar matrix on Zn metal composed of $ZnF_2/Zn_3(PO_4)_2/CF_X$ (X = 1 or 3) *via* simple electrochemical reactions in 0.5 M zinc trifluoromethane sulfonate ($Zn(OTf)_2$)-trimethyl phosphate (TEP) solution.[42] Similarly, Zhang *et al.* synthesized a PANI/carbon paste/NiTi shape memory alloy wire cathode.[43] The PANI cathode was deposited on the NiTi with a conductive carbon paste layer, using a three-electrode electrochemical deposition using a deposition current of 0.9 mA and Ag/AgCl and circular stainless-steel mesh as the reference and counter electrodes, respectively. An aqueous solution containing 0.25 M aniline and 0.5 M H_2SO_4 was used as the electrolyte. The polymerization period was 600 s, 800 s, 1000 s, and 1200 s at room temperature. Then, the obtained PANI cathode was washed with deionized water and dried under vacuum at 60 °C. Li *et al.* reported the N-MnO_2 nano-wall, which was *in situ* grown on flexible CC by electrodeposition.[44] Typically, 1.5 g of Na_2SO_4 and 2.46 g of $Mn(CH_3COO)_20.5H_2O$ were dispersed in 100 mL of deionized water and stirred for 30 min as the electrolyte. First, deposition of Mn_3O_4 on CC was carried out using a three electrode system with the Pt plate as the negative electrode, Ag/AgCl as the reference electrode, and CC as the cathode, and the deposition was carried out at 35 °C for 20 min. Then, 15 g of Na_2SO_4 was dispersed in 100 mL of deionized water and stirred at 50 °C for 30 min to prepare the electrolyte. Then, the original Mn_3O_4 on CC was activated by CV within a working voltage window of 0–1.3 V for 100 cycles. Subsequently, the sample was annealed at 200 °C in a N_2 atmosphere to obtain the N-MnO_2.

Extensive research suggests that the Zn foil anode in ZIHSCs suffers from dendritic Zn growth just like the dendrite growth problem in Li-metal electrodes during the repeated charge and discharge processes. Zn's unavoidable growth could lead to large metal dendrite formation, which can result in internal short circuits and severe safety issues.[45] To overcome this issue and increase the feasibility of ZIHSCs in practical applications, the Zn anodes are fabricated on different substrates by the electrochemical deposition method. For instance, Chen *et al.* prepared Zn@CC using a two electrode setup with a Zn plate as a counter electrode and a pre-treated CC as a working electrode in 1 M $ZnSO_4$ aqueous electrolyte.[46] The Zn deposition on CC was obtained by electroplating for 3000 s at a current density of 5 mA cm^{-2}, which was used as an anode directly in realizing practical ZIHSCs. Similarly, Lou *et al.* deposited Zn on clean CC

using a bare CC as the working electrode and Zn foil as both the reference and counter electrodes.[47] Uniform deposition of Zn on CC was achieved at a constant voltage of −1200 mV for 500 s in a 1 M $ZnSO_4$ electrolyte. Besides, Xiong *et al.* electrodeposited Zn on 3D Cu foam in an aqueous solution mixture of $ZnSO_4$, Na_2SO_4, and boric acid with 3D Cu foam and Pt used as the working electrode and counter electrodes, respectively.[40] The 3D Zn@Cu anode demonstrated improved plating/stripping efficiency and stability as compared to planar Zn foil.

3.2 Pyrolysis method

Considering a predominant, facile, and effective method for preparing carbon materials, this method has two main aspects: atmosphere and temperature, which can significantly influence the final products of the pyrolyzed precursor. Furthermore, heteroatom doping in the carbon matrix can be carried out by this method. Heteroatom sources introduced externally include non-metallic sources (nitrogen, phosphorus, sulfur, boron, *etc.*) and metal sources (iron, cobalt, copper, *etc.*). Heteroatom doping can offer multiple advantages simultaneously, including additional faradaic reactions to improve the ion storage capacity, enlarged specific surface area (SSA) to provide more reaction sites, increased electronegativity, better electrical conductivity of the host matrix, and expanded interlayer spacing to facilitate ion migration during the charge/discharge processes.[48]

3.2.1 Carbonization and nitrogenation. Carbonization is a simplistic process in which precursors are treated at high temperatures. This method extensively prepares active MOF-derived, biomass-derived, and waste material-derived porous carbon. By the carbonization method, the size and morphology of the samples can be controlled and tuned. For instance, Yang *et al.* heated as prepared ZIF-8 dodecahedra at 800 °C for 2 h in N_2 ambient to obtain N-doped carbon dodecahedra.[29] Here, *in situ* N doping in the carbon matrix occurs due to the structural N in ZIF-8. Similarly, Liu *et al.* designed porous carbon hollow spheres through a template-mediated pyrolyzation–carbonization method.[45] In detail, resorcinol and formaldehyde were used as the original precursor material to synthesize phenolic resin. Tetrapropyl orthosilicate (TPOS) was used as a templating agent to provide a silica (SiO_2) core and pore-forming particles. The initial phenolic resin and pore-forming particles co-coat on the SiO_2 core, forming SiO_2@SiO_2/RF core–shell structures which were then carbonized, followed by SiO_2 template removal to obtain mesoporous carbon hollow spheres (MCHSs) to be used as an excellent cathode in ZIHSCs. Zhang *et al.* prepared a coal tar pitch-derived porous carbon material *via* carbonizing a well-grounded mixture of coal tar pitch, aluminum phosphate, and sodium hydroxide solid in a known mass ratio in an argon atmosphere for 2 h.[49] Furthermore, Yang *et al.* reported the synthesis of coconut shell-derived activated carbon by heating crushed coconut shells at 900 °C while passing steam for 2 h.[50] Similarly, Lou *et al.* prepared poplar wood-derived carbon to use as a ZIHSC cathode.[47] 1 g of poplar wood powder, 6 mM $Zn(NO_3)_2{\cdot}6H_2O$, and 12 mM urea were properly mixed to a homogeneous powder followed by heat treatment under high-purity N_2 gas at 900 °C for 3 h with a heating ramp rate of 5 °C min^{-1}. After cooling to room temperature, the resultant mixture was washed to obtain N-doped porous carbon nanosheets. Zeng *et al.* synthesized molten salt-assisted carbon (MSPC) using ball-mill and pyrolyzation methods.[51] A mixture of 0.5 g pitch, 7.5 g NaCl and 0.25 g $NaNO_3$ was ball milled to produce a fine powder which was then pyrolyzed at 900 °C for 1 h under N_2 flow, and the resultant MSPC power was collected after washing with distilled water. In another instance, Pan *et al.* reported the synthesis of porous carbon nanoflakes for which sodium polyacrylate powder (SPA) was mixed with potassium bicarbonate powder ($KHCO_3$) and thoroughly ground in an agate mortar.[52] The mixture was then pyrolyzed in a tube furnace at 850 °C under a constant Ar flow for an hour with a heating ramp rate of 5 °C min^{-1} to carbonize and simultaneously activate the precursor to achieve porous carbon nanoflakes. Similarly, Zhou *et al.* reported the synthesis of hierarchical porous AC by high-temperature carbonization (at 900 °C) of asphalt with KOH.[53]

3.2.2 Carbonization and phosphorization. Phosphorization is the process of introducing/doping phosphorus (P) heteroatoms into carbon host materials. In this method, carbon and phosphorus sources are mixed and heat treated at high temperatures. For instance, Lee and An reported phosphorus and boron co-doped activated carbon through the pyrolysis method.[54] In detail, activated carbon (AC) was added to an aqueous solution of 1 M boric acid, 1 M red phosphorus (red P), and stirred for 3 h. The as-prepared red P and boric acid coated AC were then dried at 80 °C for 12 h in an oven followed by annealing at 800 °C for 6 h in a tube furnace under an Ar atmosphere. After annealing, the sample was washed with DI to remove residuals and obtain the desired P&B-AC. Fan and co-workers prepared P-doped honeycomb-like carbon material pyrolyzing a mixture of tannins, vanillin, phytic acid, and MgO.[55] The mixture with a known mass ratio was first treated at 180 °C for 4 h in a tube furnace in a N_2 atmosphere and further carbonized at 900 °C for 1 h at a heating rate of 5 °C min^{-1} to obtain the honeycomb-like carbons.

3.2.3 Carbonization and sulfurization. The sulfurization process during material preparation is crucial for doping sulfur (S) elements in the product. Wei *et al.* prepared N, S co-doped porous carbon from a homogenous mixture of Zanthoxylum seed cake, $KHCO_3$, and $Na_2S_2O_3$.[56] The mixture was first treated at 290 °C for 60 min in the N_2 atmosphere, then further carbonized at 800 °C for 1 h to obtain the doped product. Similarly, Wang *et al.* reported the synthesis of S-doped 3D porous carbon from sustainable pine needles for ZIHSC application.[57] The pine needle powder was first ground with C_2H_3KOS. The powder was heat treated at different temperatures for 1 h under an Ar atmosphere. The product was then neutralized with HCl, washed with DI several times, and finally dried in an oven. Yang *et al.* synthesized N, S co-doped porous carbon dodecahedra using N-doped carbon dodecahedra as the precursor material.[29] N-doped carbon dodecahedra were first synthesized *via* pyrolyzing ZIF-8 at 800 °C for 2 h in the N_2 environment. The as-obtained N-doped carbon dodecahedra

were then mixed with thiourea and again heated at 800 °C in a N_2 atmosphere with a heating rate of 5 °C min^{-1} for 2 h to obtain N, S co-doped carbon dodecahedra.

4. Electrode materials and electrolytes for ZIHSCs

4.1 Capacitor-type electrode materials

The ZIHSC's capacitor-type electrode is a crucial component. Electrode materials for capacitor-type electrodes typically consist of either carbon-based or transition metal-based compounds. These materials' specific capacity is significantly lower than battery-type electrode materials, but they are able to offer a greater rate capability and cycling stability because of their fast and reversible adsorption/desorption (or intercalation/de-intercalation) type of reaction mechanism.

4.1.1 Carbon-based materials. Carbon materials employed as the capacitor-type electrode materials in ZIHSCs possess many traits such as low-cost, abundant natural reserve and nontoxicity, rich porosity, high electrical conductivity, outstanding chemical stability in different solutions (from strongly acidic to basic), and impressive specific surface area (SSA) which are advantageous to provide an extensively large electrode/electrolyte interface for charge storage and allow fast charge movement during electrochemical reactions.[58,59]

To date, several types of carbonaceous materials have been shown to be promising cathode options for high-performance ZIHSCs. These carbons include carbon nanotubes (CNTs), graphene, porous carbon (PC), activated carbon (AC), heteroatom-doped carbons (HDC), and MOF-derived carbon. In the following subsections, we will explain the excellent electrochemical performances of ZIHSCs that are the result of carefully designed morphologies, structures, and/or controllable surface features of some recently developed carbon materials.

Graphene as cathode. Graphene is a 2D carbon-based material with high conductivity and exceptional electron mobility produced *via* the arrangement of sp^2 hybridized carbon atoms in a hexagonal honeycomb lattice. Additionally, the large theoretical specific surface area (2630 m^2 g^{-1}) and outstanding mechanical stability make it an excellent choice for many energy conversion and storage devices. Interestingly, in nanocomposites, graphene may function as a highly conducting network and a buffer layer, which can successfully prevent self-aggregation of nanoparticles and accommodate volume expansion of active materials during electrochemical processes and hence, could help in improving the cycle life and rate performance of ZIHSCs.[37,38] For instance, Zhao *et al.* synthesized N/P co-doped graphene (NPG), which exhibited a unique three-dimensional structure and a large specific surface area showing great advantages as a cathode, to assemble a Zn//NPG ZIHSC with Zn foil as the counter electrode.[32] The device could achieve a maximum energy density as high as 94.6 W h kg^{-1} and a large power density of 4500 W kg^{-1} working within a wide potential window of 1.8 V in an aqueous $ZnSO_4$ electrolyte. The device also maintained 82% capacity with almost 100% coulombic efficiency even after 15 000 cycles. Similarly, Liu *et al.* assembled ZIHSCs using a graphene cathode, flexible Zn anode, and membrane as the electrolyte.[60] At a current density of 1 A g^{-1} the device delivered a specific capacitance of 162.6 F g^{-1} at room temperature, 362.6 F g^{-1} at 80 °C, and 404.2 F g^{-1} at 100 °C. Pattananuwat *et al.* utilized a polypyrrole nanoparticle-embedded nitrogen-doped graphene composite as a novel cathode and Zn foil as the anode with 2 M $ZnSO_4$ electrolyte to fabricate a ZIHSC.[61] The SC delivered the highest capacity of 145.3 mA h g^{-1} at 0.1 A g^{-1} and maximum energy density of 232.5 W h kg^{-1} at a power density of 160 W kg^{-1} with excellent cycling stability of 85% retention after 10 000 charge/discharge cycles. Xu. *et al.* prepared p-phenylenediamine (PPD) functionalized reduced graphene oxide (RGO) film for utilization as a positive electrode in a ZIHSC with a Zn foil negative electrode.[38] This cell displayed a remarkable areal capacitance of 3012.5 mF cm^{-2} and a high energy density of 1.1 mW h cm^{-2} at a power density of 0.8 mW cm^{-2}. In another report, Jiang *et al.* assembled a flexible ZIHSC by encapsulating the redox-active phenanthraquinone (PQ)-fluffy graphene hydrogel (FGH) and Zn foil face-to-face by commercial polyethylene.[37] It achieved an areal capacity of 1.31 mA h cm^{-2} at 2 mA cm^{-2} and maintained 76.4% capacity (1 mA h cm^{-2}) when the current density was increased by 4-fold. The energy and power densities were calculated to be 1.01 mW h cm^{-2} and 1.54 mW cm^{-2}, respectively, at a current density of 2 mA cm^{-2} which outperformed many recently reported values.

Activated carbons (ACs) as cathodes. Due to its high specific surface area (SSA), abundant pores, tunable pore structure, cheap cost, and physio-chemical stability, AC has been investigated extensively as a viable and efficient electrode material for ZIHSCs.[62] Amongst others, Dong *et al.* were the first to report the successful use of a commercial AC as the cathode in a high-performance ZIHSC with Zn foil as the anode and an aqueous $ZnSO_4$ electrolyte.[26] The AC exhibited irregular morphology of particles with rough surfaces, leading to an exceptionally high SSA of 1923 m^2 g^{-1}, and resulted in a specific capacity of 121 mA h g^{-1} at 0.1 Ag^{-1}, an energy density of 84 W h kg^{-1}, and a very large power density of 14.9 kW kg^{-1}. The ZIHSC also demonstrated excellent cycling stability with 91% capacity retention after 10 000 cycles. Following that, Zhang *et al.* designed a novel form of on-chip micro ZIHSC using an AC cathode and electro-deposited Zn nanosheets as an anode material.[63] The micro ZIHSC, benefitting from its cutting-edge device design, demonstrated some impressive merits, including an areal capacitance of 1297 mF cm^{-2} at a current density of 0.16 mA cm^{-2}, which corresponds to 259.4 F g^{-1} at 0.05 A g^{-1}, an impressive energy density of 115.4 W h cm^{-2} at a power density of 0.16 mW cm^{-2}, and a long cycle life.

Although these achievements with activated carbon-based ZIHSCs are interesting, the energy density is still far from satisfactory. Therefore, exploiting low-cost, eco-friendly, and high-performance carbon materials with tunable pore structures is highly desired. In this regard, biomass-derived carbon materials have offered a variety of physicochemical properties,

including abundant reaction sites owing to their highly porous structure and surface functional groups, excellent chemical stability, and natural abundance. Such traits have made biomass-derived carbons one of the potent candidates for ZIHSC anodes. For instance, Yang *et al.* prepared coconut shell-derived activated carbon (CSAC) for its usage in ZIHSCs.[50] The activated carbons were synthesized from dried coconut shells through a simultaneous carbonization and steam activation method, as depicted in Fig. 4a. The resultant material possessed a SSA of 1260 $m^2\ g^{-1}$ and a pore volume of 1.8 $cm^3\ g^{-1}$. An aqueous ZIHSC was assembled using the natural coconut shell-derived activated carbon as the cathode, $Zn(ClO_4)_2$ as the electrolyte, and electro-deposited Zn as the anode (Fig. 4b). The aqueous ZIHSC achieved an outstanding specific capacitance of 423.5 F g^{-1} with an excellent energy density of 190.3 W h kg^{-1} at 89.8 W kg^{-1} (as shown in Fig. 4c-f). Interestingly, when anti-freezing hydrogel electrolyte replaced the aqueous $Zn(ClO_4)_2$ solution, the quasi-solid-state CSAC//PVA/MMT/$Zn(ClO_4)_2$ (gel)//Zn device maintained excellent anti-freezing properties and stability. The cycling performance of the ZIHSC device was evaluated by the GCD method over 10 000 cycles at a current density of 5 A g^{-1} which demonstrated outstanding capacitance retentions of 99% and 98% at 25 °C and at −20 °C, respectively. The results reveal excellent stability of the quasi-solid-state ZIHSC device at room and even at ultra-low temperatures. Even at temperatures as high as 60 °C, the device could still retain a specific capacitance of 80% after 5500 cycles.

Porous carbons (PCs) as cathodes. PCs have been widely explored as one of the most prospective electrode materials for ZIHSCs due to their unique properties, including a cost-effective and easy synthesis process, high surface area, large pore volume, and unique pore size distribution. Many porous carbon-based materials are available; biomass-derived porous carbonaceous materials are found to be quite attractive due to their enhanced textural properties, relatively simple and facile synthesis methods, and, more importantly, the inexpensive and renewable nature of biomass that could reduce the overall cost of the energy storage.[64,65] Pan *et al.* designed a ZIHSC with low-cost Zn metal foil, porous carbon nanoflakes, and non-corrosive $ZnSO_4$ solution as the respective anode, cathode,

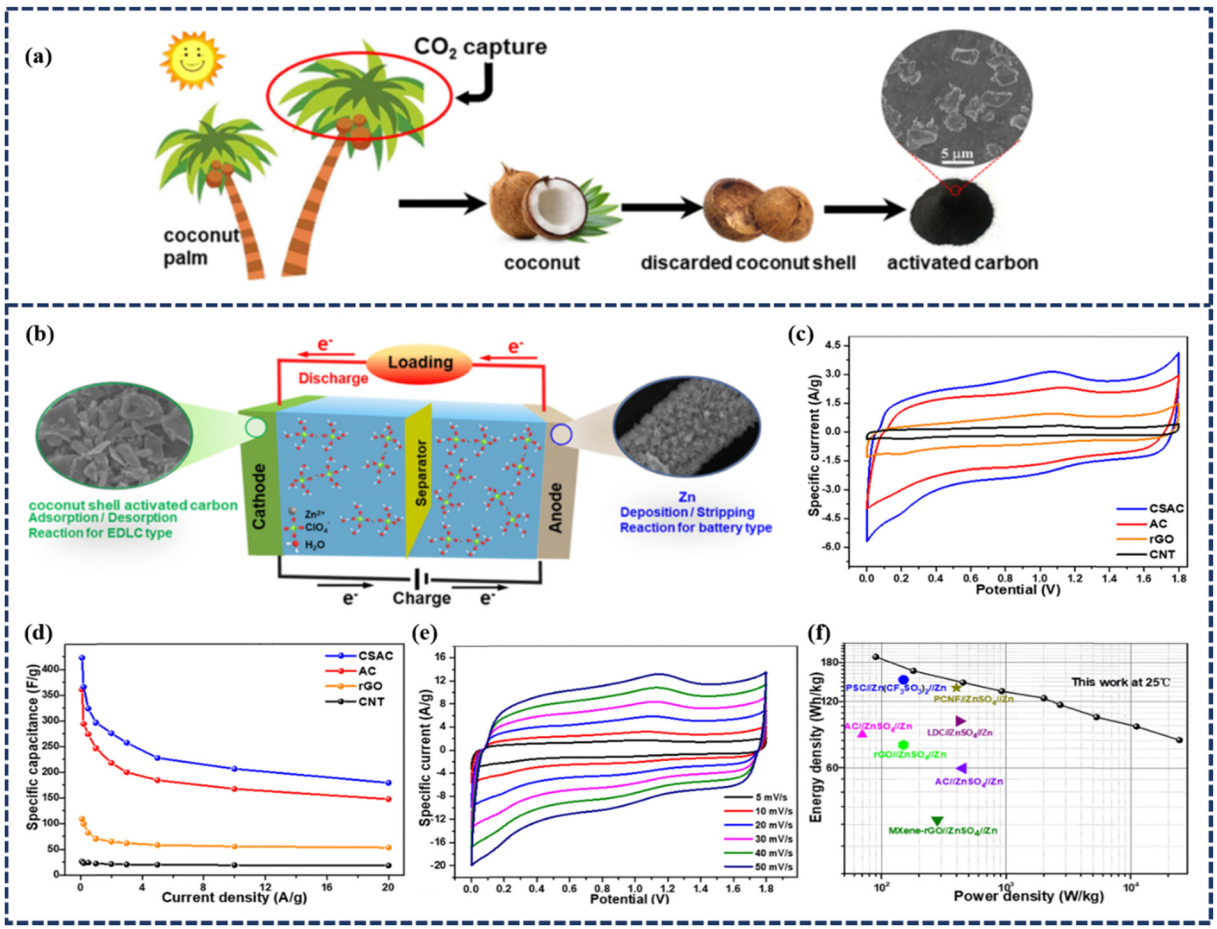

Fig. 4 (a) Schematic illustration of the coconut, coconut shell, and biochar cycle. (b) Schematic illustration of the CSAC//$Zn(ClO_4)_2$ (aq.)//Zn device. (c) CV curves of ZIHSC devices with different carbon cathodes at 10 mV s^{-1}. (d) Specific capacitance values of ZIHSC devices with different carbon cathodes at various current densities. (e) CV curves of the ZIHSC device with the CSAC cathode at different scan rates. (f) Ragone plots of the CSAC//$Zn(ClO_4)_2$ (aq.)//Zn device in comparison to other ZIHSCs at 25 °C. (Reproduced from ref. 50 with permission from Elsevier).

and electrolyte.[52] The ZIHSC demonstrated an excellent specific capacity of 177.7 mA h g^{-1} at 0.5 A g^{-1} current density and maintained 85.5 mA h g^{-1} at a high current rate of 20 A g^{-1}. Furthermore, the device achieved an energy density of 142.2 W h kg^{-1} at a power density of 400.3 W kg^{-1}. At the high power density of 15.3 kW kg^{-1}, the device delivered an energy density of 68.4 W h kg^{-1} and demonstrated a high capacity retention of 90% after 10 000 GCD cycles at a high current density of 10 A g^{-1}. Similarly, Li *et al.* presented a novel ZIHSC with excellent electrochemical performance and remarkable durability by using a pencil-shaving-derived porous carbon (denoted as PSC-A*x*, where *x* corresponds to KOH-assisted activation temperature) as a potential electrode material (as detailed in Fig. 5a).[66] To evaluate the performance of the as-prepared carbons for Zn ion storage, they constructed an aqueous ZIHSC (namely Zn//PSC-A*x*) illustrated in Fig. 5b with 1 mol L^{-1} $Zn(CF_3SO_3)_2$ as an electrolytic solution. As presented in Fig. 5b–e, Zn//PSC-A600 delivers excellent rate properties of 413.3–184.1 F g^{-1} (which correspond to specific capacities of 183.7–81.8 mA h g^{-1}) as the current density varied from 0.2 to 20 A g^{-1}. The device could also deliver a high energy density of 147.0 W h kg^{-1} at 136.1 W kg^{-1} and retained 65.4 W h kg^{-1} of energy density at a high power density of 15.7 kW kg^{-1}. This device's durability was found to be outstanding with a 92.2% capacity retention observed during 10 000 cycles at 10 A g^{-1} (Fig. 5f), and can be credited to the excellent chemical stability of the porous carbon materials. Furthermore, Zhou *et al.* reported an aqueous ZIHSC with a hierarchical porous AC

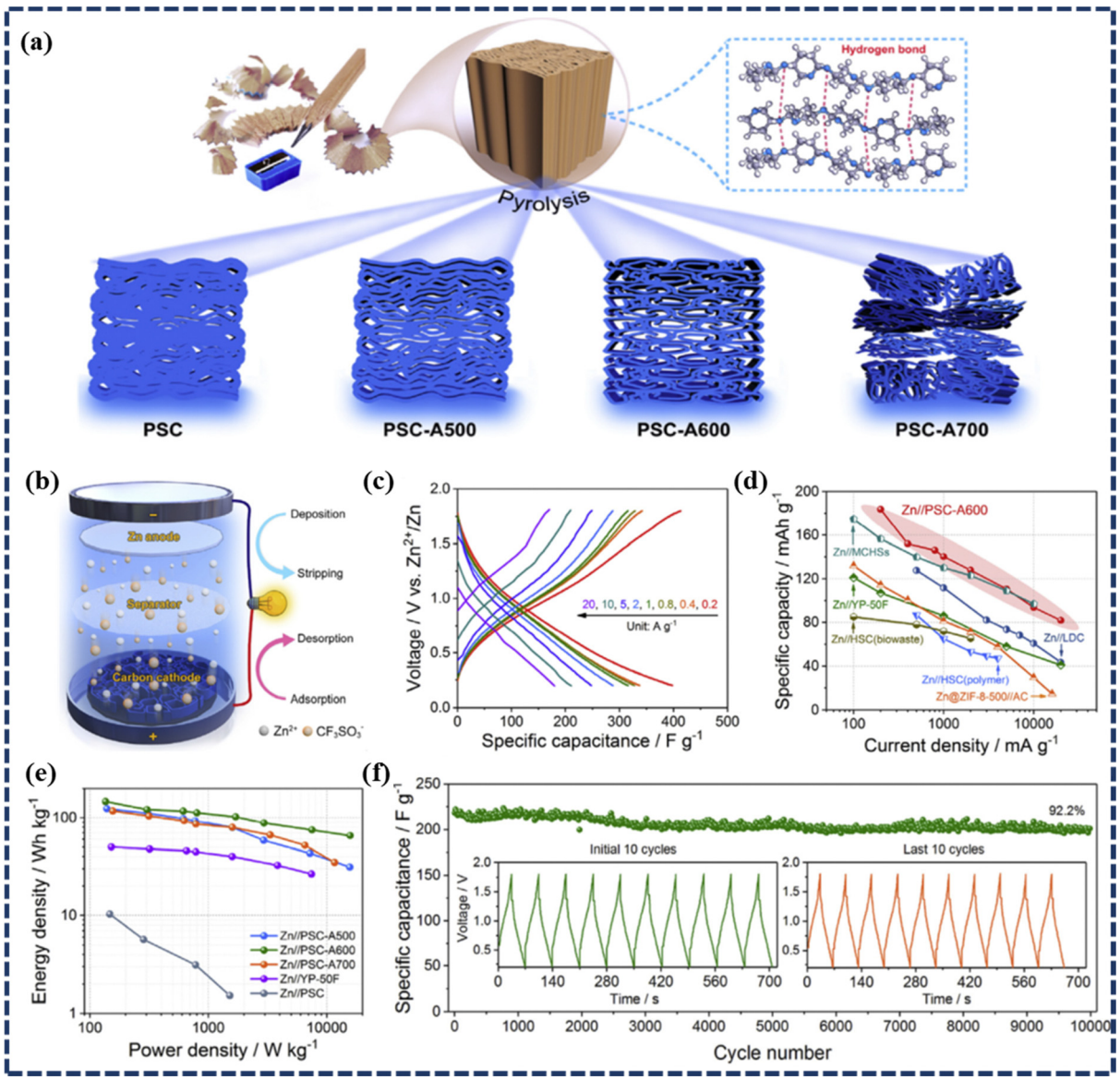

Fig. 5 (a) Schematic diagram of the synthesis of PSC and PSC-A*x* (PSC-A500, PSC-A600, and PSC-A700), (b) schematic model of the ZHSC energy storage system, (c) GCD profiles of the PSC-A600 at different current densities, (d) a comparison of the rate performance between PSC-A600 and other carbon materials reported for ZIHSCs, (e) Ragone plots for different PSC-based devices, and (f) cycling performance test of the device over 10 000 GCD cycles, with the initial and last 10 GCD profiles as the inset (reproduced from ref. 66 with permission from Elsevier).

(HPAC) as the cathode, and 3 M $Zn(CF_3SO_3)_2$ and Zn foil as the respective electrolyte and anode.[53] Interestingly, at 0.5 A g^{-1} current density, the specific capacity of the device was as high as 231.0 mA h g^{-1}, and it still delivered a high capacity of 119.4 mA h g^{-1} even at the ultra-high current density of 20 A g^{-1}. Such performance is at par with the best-reported Li-free hybrid energy storage devices based on carbon cathodes. Moreover, the ZIHSC exhibited a high energy density, particularly at high power density (77.5 W h kg^{-1} at 11.4 kW kg^{-1}) and long cycle life with a capacity retention of 70% after 18 000 cycles at 10 A g^{-1}. Yau *et al.* used sweet messes from glutinous rice alcoholic fermentation as an abundant green carbon source to prepare a new porous carbon material by mixing the biomass with KOH followed by carbonization in a N_2 atmosphere.[67] Subsequently, a carbon-based ZIHSC was assembled with prepared PC (with a high micropore area of 1991 m^2 g^{-1}) as the cathode and Zn foil and 2 M $ZnSO_4$ as the anode and electrolyte, respectively. This device offered an ultrahigh energy density of 116 W h kg^{-1} at a power density of 800 W kg^{-1}. In addition, the device showed a long lifetime over 270 000 charge/discharge cycles with ~100% coulombic efficiency. T. Xiong *et al.* assembled a ZIHSC by using MOF-derived porous carbon as a cathode and electrodeposited Zn on Cu foam as the anode with 1 M $ZnSO_4$ electrolyte. This assembled cell demonstrated a maximum energy density of 36.4 W h kg^{-1}, exceptional power density of 85.5 kW kg^{-1}, and 99% capacity retention after 20 000 cycles.[40]

Heteroatom-doped carbons as cathodes. Heteroatom doping into carbon materials is crucial to tailor their electron-donor properties and consequently tune their electrical and electrochemical performance. Incorporating heteroatoms into the carbon surface has been shown to significantly enhance several properties of nanocarbon, such as the porosity, electrochemically active sites, charge density, charge distribution, wettability, interlayer spacing, electrical conductivity, and pseudocapacitance leading to significant enhancement of the supercapacitive performance of the carbon structures.[68–70] Considering these unique advantages, recently, heteroatom-doped carbons have been identified as promising electrode materials for ZIHSCs. For instance, Lu *et al.* reported layered B/N co-doped porous carbon (LDC) using an intercalator (H_3BO_3)-guided pyrolysis technique.[71] The LDC was used as a cathode in an aqueous Zn//$ZnSO_4$ (aq.)//LDC ZIHSC device for the first time, which delivered a specific capacity value of 127.7 mA h g^{-1} at 0.5 A g^{-1} and retained 42.8 mA h g^{-1} at 20 A g^{-1}. The maximum energy density and power density obtained for the LDC-based ZIHSC were 97.6 W h kg^{-1} and 12.1 kW kg^{-1}, respectively. Furthermore, driven by the good performance of the aqueous ZIHSC, a quasi-solid-state Zn//gelatin/$ZnSO_4$ (gel)//LDC ZIHSC was further assembled and demonstrated. This solid-state device achieved a specific capacity of 116.8 mA h g^{-1} at 0.5 Ag^{-1} with a retention of 55.4 mA h g^{-1} capacity at a high current rate of 20 A g^{-1}. A maximum energy density of 86.8 W h kg^{-1} was achieved with a power density of 429.6 W kg^{-1} at 0.5 Ag^{-1} current density. On the other hand, at a maximum power density of 12.1 kW kg^{-1}, the energy density was 25 W h kg^{-1}. The quasi-solid-state ZIHSC also demonstrated long-term cycling durability, with 81.3% capacity retention over 6500 cycles observed at 5 A g^{-1} with 100% coulombic efficiency. Furthermore, Zhang *et al.* prepared N & P co-incorporated porous carbon nanosheets (CNPK) for their usage as a novel cathode material for ZIHSCs.[72] Density functional theory (DFT) calculations revealed that the N & P co-doping could reduce the reaction energy barrier between Zn^{2+} ions and the cathode promoting the Zn-ion adsorption and resulting in superior performance. The electrochemical performances were tested in a three-electrode system using Ag/AgCl as a reference electrode and Pt foil as a counter electrode in 1 M $ZnSO_4$ electrolyte, which demonstrated that the N & P co-doped CNPK could deliver a specific capacity of 103.2 mA h g^{-1} (232.2 F g^{-1}) at 0.1 A g^{-1}, an energy density of 81.1 W h kg^{-1}, a power density of 13.366 kW kg^{-1}, and superior cycling stability with 101.8% capacitance retention after 10 000 cycles. Furthermore, for practical applications, a quasi-solid-state ZIHSC was assembled, which delivered a high capacity of 141.0 mA h g^{-1} at 0.1 A g^{-1} and an outstanding energy density of 89.3 W h kg^{-1}. Yang *et al.* prepared zeolitic imidazolate framework (ZIF)-derived N, S co-doped porous carbon dodecahedra (N, S-PCD) for use as a high-performance cathode in an aqueous ZIHSC with ultra-long cycle life.[29] The synthesis method comprises pyrolyzation of ZIF-8 in an inert atmosphere followed by sulfurization, as shown in Fig. 6a. Here, the N-doping in the carbon matrix occurred *in situ* from the structural N of ZIF-8 during the carbonization step. Benefitting from the hierarchical porous structure of nanocarbon and N, S dual-doping offering numerous reaction sites, the as-assembled Zn//N, S-PCD ZIHSC produces a maximum specific capacity of 133.4 mA h g^{-1} (300.2 F g^{-1}) at 0.2 A g^{-1} current density, which corresponds to an outstanding energy density of 106.7 W h kg^{-1} at the power density of 160 W kg^{-1} (Fig. 6b–e). Besides, outstanding cycling stability has also been observed with 97.1% capacity retention during 100 000 charge–discharge cycles (Fig. 6f), indicating superior stability of the electrode materials beneficial for practical applications. Similarly, Wang *et al.* explored the Zn-ion storage performance of N & P co-doped onion-like carbon (N, P-OLC) as a cathode material in ZIHSCs.[73] Notably, the ZIHSCs assembled with N, P-OLC as the cathode, and Zn foil as the anode could achieve a high specific capacitance of 420.3 F g^{-1} (equivalent capacity 184.5 mA h g^{-1}) at a current density of 0.5 A g^{-1}, and retained 262.7 F g^{-1} (~63% capacitance retention) even at a high current density of 20 A g^{-1}. Such performance of N, P-OLC-based ZIHSCs is reported to be far better than most of the previously reported AC and PC-based ZIHSCs. Moreover, the N, P-OLC was *in situ* tightly integrated with carbon cloth (CC) to fabricate a flexible electrode, which was then coupled with a Zn anode to realize a quasi-solid state Zn//N,POLC@CC device. Interestingly, this fiber-shaped flexible device achieved a high energy of 85.3 mW h cm^{-2} and a superior power of 24.3 W cm^{-2}, along with an excellent durability of ~77.8% capacitance retention over 50 000 cycles. The device also demonstrated excellent flexibility and practicality indicating the high potential of OLCs for high-performance ZIHSCs. Wei *et al.* assembled a ZIHSC by using N-doped porous carbon derived from ZIF-8 MOF as the cathode

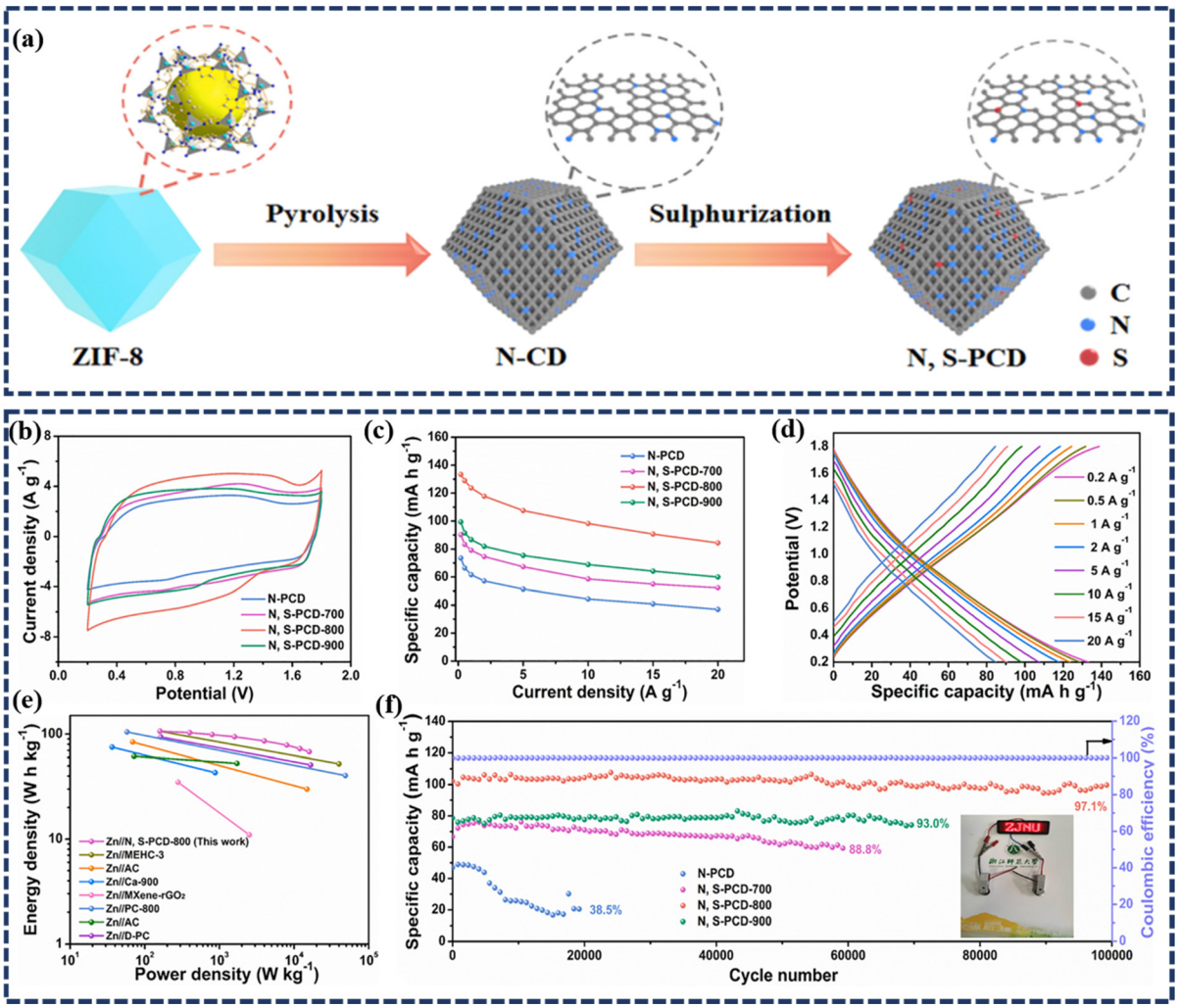

Fig. 6 (a) Schematic diagram of the preparation of N, S-PCD *via* a two-step process; (b) CV curves at 20 mV s^{-1} and (c) specific capacities at different current densities of the as-prepared N-PCD, N, S-PCD-700, N, S-PCD-800, and N, S-PCD-900 samples, respectively; (d) GCD curves of N, S-PCD-800 at different current densities from 0.2 to 20 A g^{-1}; (e) Ragone plot of the Zn//N, S-PCD-800 ZIHSC in comparison with some recently reported ZIHSCs; (f) the cycling performance of ZIHSCs at a current density of 5 A g^{-1} and the coulombic efficiency of N, S-PCD-800; the inset depicts a digital picture of LEDs illuminated by two coin-type Zn//N, S-PCD-800 ZIHSCs in series. (Reproduced from ref. 29 with permission from Elsevier).

and Zn foil as the anode.[39] The assembled ZIHSC could deliver a maximum energy density of 121.2 W h kg^{-1}, and an excellent power density of 16 kW kg^{-1}, along with a stable cycling performance with over 75% capacity retention after 20 000 cycles, suggesting numerous possibilities with heteroatom rich porous carbon structures as a next-generation ZIHSC cathode.

Conducting polymer-based materials as cathodes. Conducting polymers (CPs) are pseudocapacitive materials that store energy through fast and reversible faradaic redox reaction on the surface of the electrode materials and at the vicinity of the electrode–electrolyte interface, and provide far higher capacitance than carbon-based materials. However, most of the conducting polymers show poor cycling stability due to continuous swelling/shrinkage cycles during the charge/discharge processes, which hinders their practical applications as electrode materials. Therefore, the synthesis of CP/carbon and CP/metal oxide composites is a practical approach to overcome the problem because two components in the composites can improve the energy storage performance through synergy. Representative conductive polymers include polypyrrole, polyacetylene, polyaniline, polythiophene, and poly(3,4-ethylenedioxythiophene) polystyrene sulfonate. These materials are widely used in hybrid supercapacitors and rechargeable batteries due to merits such as easy fabrication, controllable structures, flexibility, and high electrical conductivity.[74,75]

In recent years, investigations on CP or CP-based composite electrode materials as cathodes in ZIHSCs have been reported. For instance, Wang *et al.* electrodeposited polymer poly(3,3′-dihydroxybenzidine, DHB) on porous active carbon (AC) granules.[76] A flexible sandwich-structured cell was constructed that combines the Zn foil anode and the poly(3,3′-DHB)/AC composite as the cathode. This cell delivered an areal capacitance of 1.3 F cm^{-2} with maximum energy and power densities

of 0.18 mW h cm^{-2} and 4.01 mW cm^{-2}, respectively. The cell demonstrated stable electrochemical performance upon bending, indicating application potential in flexible devices. To further improve the performance of ZIHSC, Xin *et al.* designed an aqueous Zn//poly(4,4′-TDP)/AC cell by using electrodeposited poly(4,4′-thiodiphenol) on a porous AC cathode and Zn anode, as schematically demonstrated in Fig. 7a.[77] In Fig. 7b, the Zn//poly(4,4′-TDP)/AC cell demonstrated stable electrochemical performance within a wide potential window of 0.1–1.9 V as represented by the CV curves at different scan rates. In comparison, the normal Zn//AC hybrid supercapacitor had a voltage window of 0.2–1.8 V and a poor capacitance value with a narrower area under the CV curve (Fig. 7c). This indicates that the introduction of poly(4,4′-TDP) into the AC enhances not only the capacitance of the cathode but also the operational voltage window, and hence an increased energy density too. This is because of the additional faradaic processes introduced by both the Zn^{2+} and H^{+} ions bound to the carbonyl groups of the poly(4,4′-TDP) polymer and the insertion/de-insertion of the H^{+} ions during the charge storage. According to the GCD cycling test of the Zn//poly(4,4′-TDP)/AC cell at 8 mA cm^{-2}, it retains 71% capacity after 2000 cycles (as shown in Fig. 7d). As per the GCD data in Fig. 7e, a maximum areal capacity of 0.85 mA h cm^{-2} (~188 mA h g^{-1}) could be obtained. However, from the practical application point of view, higher mass loading is better for achieving higher energy density. In Fig. 7f, the rate capabilities of Zn//poly(4,4′-TDP)/AC devices with different mass loading of the cathode material are demonstrated. Here, the capacity first increases with increasing mass loading and reaches saturation when the cathode mass loading is beyond 5 mg cm^{-2}, which can be attributed to the limited permeation depth of poly(4,4′-TDP) electrodeposited on AC. For the device with a cathode mass loading of 5 mg cm^{-2}, an areal capacity of 1.2 mA h cm^{-2} at 1 mA cm^{-2} was achieved. Furthermore, the maximum areal energy density of 1.03 mW h cm^{-2} at a power density of 0.9 mW cm^{-2} was achieved from the cell with the thickest AC coating in the cathode. In Fig. 7g, Ragone plots for the Zn//poly (4,4′-TDP)/AC cells of different cathode mass

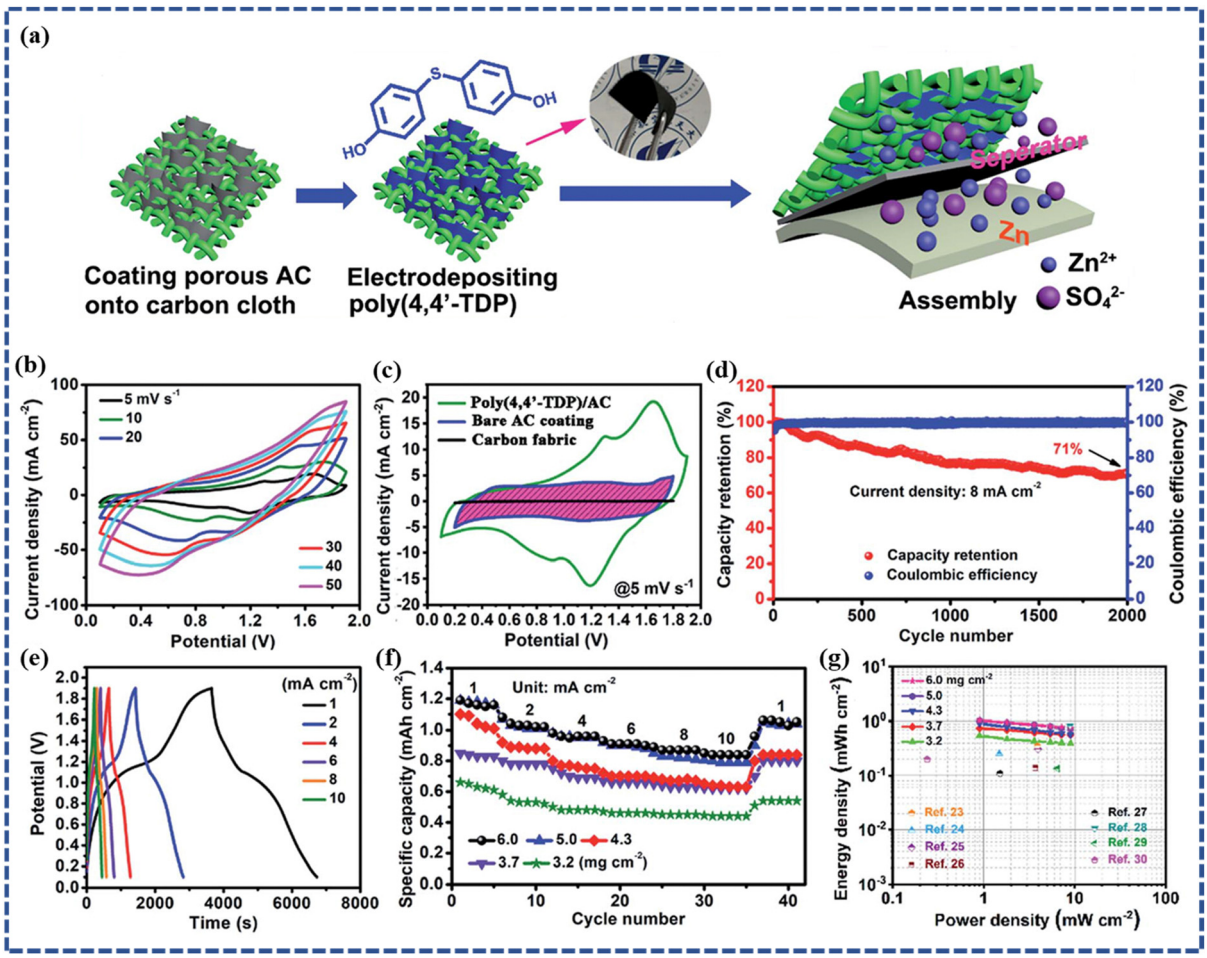

Fig. 7 (a) Diagram of the synthesis process of a Zn//poly(4,4′-TDP)/AC cell, (b) CV curves of the Zn//poly (4,4′ -TDP)/AC cell at different scan rates, (c) CV curves collected from three cells using bare carbon fabric, bare AC coating, and poly(4,4′-TDP)-modified AC coating as the cathodes, respectively, (d) cycling stability of the Zn//poly(4,4′-TDP)/AC cell, (e) GCD curves at different current densities, (f) rate performances of a group of Zn//poly(4,4′-TDP)/AC cells with different AC mass loadings in the cathode, (g) comparison of the Ragone plots of the Zn//poly(4,4′-TDP)/AC cells with some other ZIHSC devices reported recently. (Reproduced from ref. 77 with permission from Royal Society of Chemistry).

loadings were reported and compared with some of the other recently reported ZIHSCs where the superiority of the Zn//poly(4,4′-TDP)/AC devices could be observed clearly. Similarly, Cui *et al.* synthesized polyacrylamide and porphyrin-based polymer POP-TAPP-NTCA as a new electrode material for ZIHSC.[78] Firstly, the ZIHSC device was assembled with POP-TAPP-NTCA as the anode and EG/PANI as the cathode in a 2 M $ZnSO_4$ aqueous electrolyte. Based on the GCD tests, the specific capacitances of ZIHSC at the current densities of 0.13, 0.18, 0.3, 0.6, 1.13, and 1.5 A g^{-1} were found to be 172, 158, 147, 129, 107, and 94 F g^{-1}, respectively. Based on the total mass of the active anode and cathode materials, the specific energy density of the ZIHSC was calculated to be 48 W h kg^{-1} at a specific power density of 85 W kg^{-1}. Another attractive feature of the fabricated ZIHSC device was its excellent cycling stability. The fabricated ZIHSC device demonstrated a high capacitance retention of 90% after 1100 charge/discharge cycles. Tung *et al.* presented the application of the polyaniline (PANi)/Mn-Fe binary metal hydroxide (MnFe-BMH) composite as a cathode and Zn as the anode material in a ZIHSC.[79] The ZIHSC cell was assembled with a gel electrolyte composed of 1 M $ZnSO_4$ and 0.1 M $MnSO_4$. This ZIHSC achieved a superb specific capacitance of 470.3 F g^{-1} with an outstanding energy density of 167 W h kg^{-1} at a scan rate of 5 mV s^{-1}. Furthermore, the prepared MnFe-BMH composite electrode also showed good cycling stability by retaining 94.6% of the first cycle capacity after 11 602 cycles. In another instance, Zhang *et al.* assembled aqueous ZIHSC using PANI/NiTi-800 as a cathode and Zn wire as an anode, which delivered the energy density of 55.9 W h kg^{-1} at a current density of 5 A g^{-1} and excellent cycle stability with 80% capacity retention after 5000 cycles.[43]

MXene-based materials as cathodes. MXenes are a few atom thick transition metal carbides, nitrides, or carbonitrides. They are emerging as promising 2D electrode materials due to a variety of intrinsic properties, including high intrinsic electronic conductivity, rich surface chemistry, good hydrophilic nature, and outstanding flexibility. Besides these, owing to their good pseudocapacitive behavior in protic electrolytes, and abundant electrochemically active sites for ion adsorption and intercalation, MXenes have inspired the design of Zn-MXene capacitors that utilize an acidic electrolyte, such as $ZnSO_4$, to facilitate high-rate electrochemical intercalation of Zn^{2+} ions.[13,80–83] Thus, a large pseudocapacitance could be obtained with MXene-based electrodes, making it a more energetically suitable capacitor-type cathode material for ZIHSCs in comparison to other AC and/or PC-based electrodes. For instance, Yang *et al.* prepared a Zn@Ti_3C_2 anode and Ti_3C_2 cathode to systemically examine their electrochemical performance as a rechargeable ZIHSC in the presence of a gel electrolyte.[84] This ZIHSC achieved a volumetric capacitance of 330 F cm^{-3} (equivalent specific capacitance of 132 F g^{-1}) at 0.5 A g^{-1} current density along with a high-rate capability of 91.6% when the current density was increased to about 3 A g^{-1}. The cell also exhibited a good cycling performance by sustaining 82.5% of the specific capacitance after 1000 cycles measured at 3 A g^{-1}. Similarly, Li *et al.* reported a zinc-ion hybrid micro-supercapacitor (ZIHMSC) using polyacrylamide (PAM)/$ZnSO_4$ hydrogel electrolyte, $Ti_3C_2T_x$ MXene as the capacitor-type anode, and vanadium pentoxide (V_2O_5) as the battery-type cathode.[85] This zinc ion micro supercapacitor has demonstrated excellent electrochemical characteristics with a high energy density of 48.9 μW h cm^{-2} at a power density of 673 μW cm^{-2}, a high areal capacitance of 129 mF cm^{-2} at a current of 0.34 mA cm^{-2}, and a stable cycling performance with 77% capacitance retention after 10 000 cycles. In another study, Mao *et al.* reported a degradable micro ZIHSC based on a MXene/$ZnCl_2$ anode and MnO_2-MWCNTs cathode.[86] To overcome the problem regarding poor Zn-ion storage capacitance of MXenes, the $ZnCl_2$ modification strategy was used for pre-intercalation of Zn^{2+} ions into the layer of MXenes through osmotic pressure, thus opening more active sites for the subsequent fast Zn^{2+} intercalation. It was also mentioned that a part of the –F terminals on the surface of MXene would also get replaced by the Cl^- ions in this process. In Fig. 8a, the optical photographs of MXene/$ZnCl_2$ and MnO_2-MWCNTs are shown. A comparison of the CV curves of the anode and cathode materials is shown in Fig. 8b at a scan rate of 1 mV s^{-1}, implying a good charge balancing between the anode and cathode, which is a crucial factor in achieving the optimum performance of the device. Fig. 8c shows the CV curves of the ZIHSC exhibiting typical redox peaks and large current densities at various scan rates ranging from 1 to 50 mV s^{-1} indicating dominant redox activity of the electrode materials. Then, the GCD curves of ZIHSC at different currents ranging from 0.2 A g^{-1} to 10 A g^{-1} were recorded and analyzed. As shown in Fig. 8d, almost-symmetric charge–discharge profiles at different current densities demonstrate good electrochemical performance and excellent reversibility of the assembled ZIHSC. Furthermore, the ZIHSC achieved a good specific capacitance as high as 194.1 F g^{-1} at 1 mV s^{-1} and even retained 56.4 F g^{-1} at 50 mV s^{-1} (as shown in Fig. 8e). The Ragone plot in Fig. 8f demonstrates that the energy and power densities of the assembled cell could reach 90.1 W h kg^{-1} and 9250 W kg^{-1}, respectively, which are higher than several other ZIHSCs. The cycling performance of the ZIHSC was also remarkable, with 86.9% capacitance retention and almost 100% coulombic efficiency during 12 000 cycles measured at 10 A g^{-1} (Fig. 8h).

Other capacitor-type materials. In addition to the capacitor-type electrode materials listed above, phosphorene, titanium nitride (TiN), diamond fibers, and few-layer siloxane have been used as cathode materials for realizing high-performance ZIHSCs.[87] For instance, Huang *et al.* assembled various phosphorene (BP)-based ZIHSCs by utilizing "water in salt" (WIS) or propylene carbonate (Et_4NBF_4/PC) electrolytes.[88] The Zn-BP-WIS ZIHSC operates in a voltage range of 2.2 V and delivers a specific capacitance of 304 F g^{-1} at 0.2 A g^{-1} and an excellent rate performance with 145.9 F g^{-1} at 6.4 A g^{-1}, while the Zn-BP-PC ZIHSC operates in the potential window of 2.5 V and presents a high specific capacitance of 363.9 F g^{-1} at 0.2 A g^{-1} and 46.1 F g^{-1} at 6.4 A g^{-1}, respectively. Moreover, the phosphorene-based ZIHSCs have outstanding anti-self-discharge

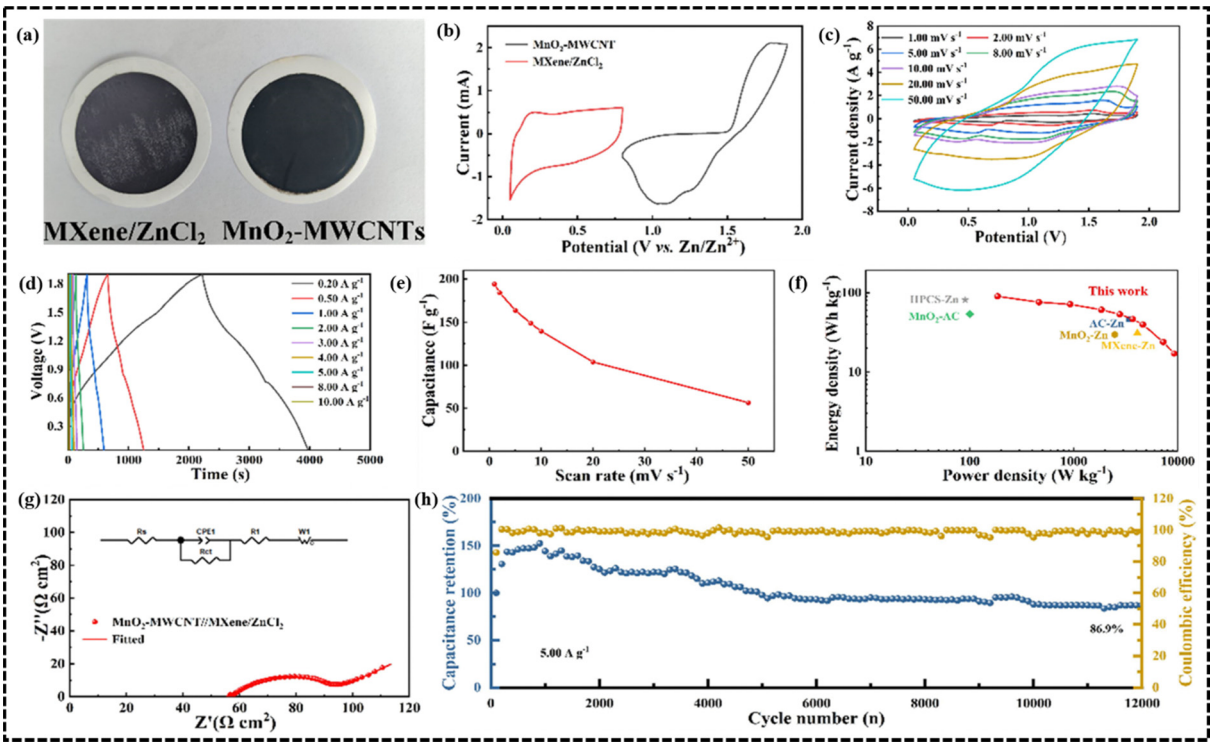

Fig. 8 The electrochemical performance of the MXene/$ZnCl_2$//MnO_2-MWCNTs ZIHSC. (a) Digital photographs of the cathode and anode, (b) CV curves at a scan rate of 1 mV s^{-1}, (c) CV curves of the device at different scan rates, (d) GCD curves of the device at different current densities, (e) plot of rate performance, (f) Ragone plot, (g) Nyquist plot (inset is a fitted circuit diagram) and (h) cycling performance of the assembled ZIHSC. (Reproduced from ref. 86 with permission from Elsevier).

abilities with 76.16% capacitance retention after 300 h testing time. Similarly, Huang *et al.* fabricated a Zn//$ZnSO_4$//TiN ZIHSC, which delivers a very high specific capacitance of 489.8 F g^{-1} at 0.2 A g^{-1} and 314.5 F g^{-1} (1 A g^{-1}) after 10 000 charge/discharge cycles.[89] More importantly, the ZIHSC exhibits unique anti-self-discharge capability with 83.92% capacitance retention even after testing for 500 h. Jian *et al.* assembled a flexible ZIHSC using diamond fibers (DFs) as the cathode and Zn nanosheet coated DFs as the anode, which presented a high gravimetric specific capacitance of 246.1 F g^{-1} at 0.2 A g^{-1}, and a remarkable energy density and power density of 70.7 W h kg^{-1} and 4.39 kW kg^{-1}, respectively.[90] Additionally, it continued to demonstrate superior gravimetric and volumetric power and energy density under a variety of bending deformation conductions. Meanwhile, Guo *et al.* designed a few-layer siloxane nanosheet-based ZIHSC, which could deliver a maximum areal capacitance of 6.86 mF cm^{-2}, a maximum energy density of 10.66 mJ cm^{-2}, a high power density of 4.50 mW cm^{-2}, and long cycling stability with 94.3% capacitance retention after 16 000 cycles.[91]

4.1.2 Transition metal-based oxides as cathodes. Transition metal oxides (TMOs) have been extensively investigated in energy storage devices because of their natural abundance, cost-effectiveness, and multiple valencies of metal ions endowing rich redox reactions. TMOs have obtained much interest in the category of active pseudocapacitive materials owing to their excellent redox properties resulting in much higher energy density as compared to EDLC-based electrodes. TMOs store and release charges *via* highly reversible redox reactions at and/or near the electrode–electrolyte interface. Because of such advantageous traits, TMOs have also been used as the cathode materials for assembling a second-type (Type-II) of ZIHSCs.[92,93] In this regard, the most comprehensively investigated pseudocapacitive TMO compounds are RuO_2 and MnO_2-based. For Zn-ion storage, Dong *et al.*[94] presented a $RuO_2{\cdot}H_2O$//Zn ZIHSC with $Zn(CF_3SO_3)_2$ as the electrolyte, which could offer a potential window of 0.4–1.6 V. Benefitting from the large pseudocapacitance of $RuO_2{\cdot}H_2O$, this ZIHSC produced a high specific capacity of 122 mA h g^{-1} (0.1 A g^{-1}), a high energy density (82 W h kg^{-1}), an ultrahigh power density (16.74 kW kg^{-1}), and excellent cycling stability with 87.5% capacity retention over 10 000 cycles. In another report, Chen *et al.* used Zn_xMnO_2 nanowires of tunnel-like structure as a cathode and activated carbon cloth (ACC) as an anode to realize a Zn_xMnO_2//ACC ZIHSC in an aqueous electrolyte solution composed of 2 M $ZnSO_4$ and 0.4 M $MnSO_4$.[95] This ZIHSC achieved an areal capacitance of 1745.8 mF cm^{-2} (equivalent gravimetric capacitance of 145.5 F g^{-1}) at 2 mA cm^{-2}, a remarkable areal energy density of 969.9 μW h cm^{-2}, and a good cycling stability with 83.1% capacity retention after 5000 cycles measured at a high current density of 15 mA cm^{-2}.

Although TMOs have proved themselves to be strong contenders for high-performance ZIHSCs, the research on TMOs in ZIHSCs is still limited because of the significant electrochemical stability-related issues these TMOs bring up. As a

result, additional electrode materials based on other insertion-type pseudocapacitive TMOs, especially niobium oxide, vanadium oxides, and manganese oxides, can be investigated extensively as ZIHSC electrodes. Strategies for stabilizing their layered or tunnel-like structures and reducing the production of by-products are also strongly advised in this regard.

4.2 Battery-type electrode materials

Besides the capacitor-type cathode, the battery-type electrode material plays a major role in determining the energy density of the whole hybrid supercapacitor device. Planar Zn foils, Zn nanostructures, transition metal oxides (such as manganese- and vanadium-based oxides), transition metal phosphides, titanium-based sulfides, *etc.*, are the main battery-type electrode materials used in ZIHSCs. Due to the varied charge storage mechanisms, as described in Section 2.2, the battery-type electrode materials may provide a larger specific capacitance than the capacitor-type electrode materials. However, limited by the sluggish reaction kinetics, the battery-type electrode materials have an impact on the power density and cycling stability of the hybrid energy storage devices.[87]

4.2.1 Zinc metal. Due to its broad working potential window, superior chemical stability, earth-abundant nature, cost-effectiveness, environmental friendliness, high theoretical specific ($\sim$ 820 mA h g^{-1}) and volumetric (5855 mA h cm^{-3}) capacities, and suitable redox potential (−0.76 V *vs.* SHE), metallic Zn foil has been used most often as an anode material in ZIHSCs. However, there are several drawbacks associated with metal Zn anodes that are difficult to avoid in practical devices, such as uncontrolled Zn dendrite formation and growth, unbearable hydrogen evolution reaction (HER), and undesirable spontaneous Zn corrosion. These drawbacks have substantially limited the practical feasibility of ZIHSCs on a large scale. Therefore, significant efforts have been expended to resolve these problems, and several ingenious techniques, including Zn surface modification, rational design of the Zn metal anode, and electrolyte optimization, are found to be appropriate.

Modification of the Zn electrode. By enabling a uniform distribution of the surface electric field and enhancing the capacity of Zn ions to diffuse, surface modification techniques and design of nanostructured Zn electrodes may successfully prevent the production of Zn dendrites. In this regard, the carbon coating method can slow down the growth of Zn dendrites by decreasing the local current density, and hence, can prevent the development of unwanted side reactions. For instance, Liu *et al.* reported mesoporous carbon hollow spheres (MCHSs) coated on Zn foil (Fig. 9a) and used as the anode for a ZIHSC, while as-synthesized MCHSs were used as the cathode.[45] It's been observed that the excellent nanostructure of MCHSs not only provides better double-layer performance but also reduces and regulates the Zn dendrite formation. This MCHS//MCHS@Zn supercapacitor device exhibited a high energy density of 129.3 W h kg^{-1} at a power density of 266.4 W kg^{-1} and a high power density of 13.7 kW kg^{-1} at an energy density of 36.8 W h kg^{-1}. The device also demonstrated outstanding cycling performance with 100% capacitance retention after 1000 cycles and 96% after 10 000 cycles at 1 A g^{-1} current density. Han *et al.* were the first to show that covering the Zn surface with a metallic indium (In) layer that serves as both a nucleating agent and a corrosion inhibitor is a simple but efficient way to prevent dendritic formation and drastic corrosion.[96] Zn|In//Zn|In symmetric cells were assembled, which showed an extremely small voltage hysteresis of 54 mV for over 1500 h of repeated plating/stripping cycles. Furthermore, the cycling stability of the Zn|In//Zn|In symmetric cell was found to be almost 49 times better than the Zn//Zn symmetric cell observed for over 500 h. It is argued that the In layer played a crucial role in increasing the HER overpotential and providing a homogeneous Zn^{2+} flux along with a low local current density to subdue the dendrite formation and corrosion.

On the other hand, Zhang *et al.* produced an on-chip ZIHMSC by assembling a Zn nanosheet anode and AC cathode with a 2 M $ZnSO_4$ aqueous electrolyte. The device showed excellent electrochemical performance with an exceptional areal capacitance of 1297 mF cm^{-2} (at 0.16 mA cm^{-2} current density), a remarkable areal energy density of 115.4 μW h cm^{-2}, and striking cycling stability without obvious attenuation of the capacity over 10 000 cycles.[63] The energy storage mechanism of ZIHMSC with the AC cathode and electro-deposited Zn nanosheet anode was extensively examined *via ex situ* XRD and SEM techniques at different charge/discharge stages. The experimental results demonstrate that the Zn nanosheet anode maintains its crystal structure and morphology even after 50 charge/discharge cycles and that the vertical porous nanosheets effectively limit Zn dendrite seed growth, leading to high Zn stripping/plating efficiency and cycling stability of the ZIHMSC. Similarly, An *et al.* prepared a controlled electroplated 2D-Zn metal electrode (Fig. 9b), which boosts ion diffusion and energy storage.[97] The 2D-Zn//AC ZIHSC reached a specific capacitance of 468 F g^{-1} at a current density of 0.5 A g^{-1} and maintained 150 F g^{-1} at 20 A g^{-1}. The device also achieved a high energy density of 208 W h kg^{-1} at a power density of 500 W kg^{-1} and a maximum power density of 20 000 W kg^{-1} at an energy density of 66 W h kg^{-1}. This ZIHSC also demonstrated outstanding cycling performance with a capacitance retention of 99%, even over 10 000 charge/discharge cycles.

4.2.2 Transition metal-based materials

Manganese-based oxides. Manganese-based oxides as battery-type electrode materials have drawn significant interest due to their cheap cost, high theoretical capacity, environmental friendliness, low toxicity, and variety of valence states (Mn^0, Mn^{2+}, Mn^{3+}, Mn^{4+}, Mn^{7+}) desirable for a low-cost and high-performance cathode material. The charge storage in manganese oxides is dominantly pseudocapacitive in nature and credited to sequential and reversible transitions between different valence states during charge/discharge cycles. Therefore, various morphologies and nanostructures of manganese-based oxides, particularly MnO_2, as cathodes in ZIHSCs have been thoroughly studied. For example, Ma *et al.* designed MnO_2

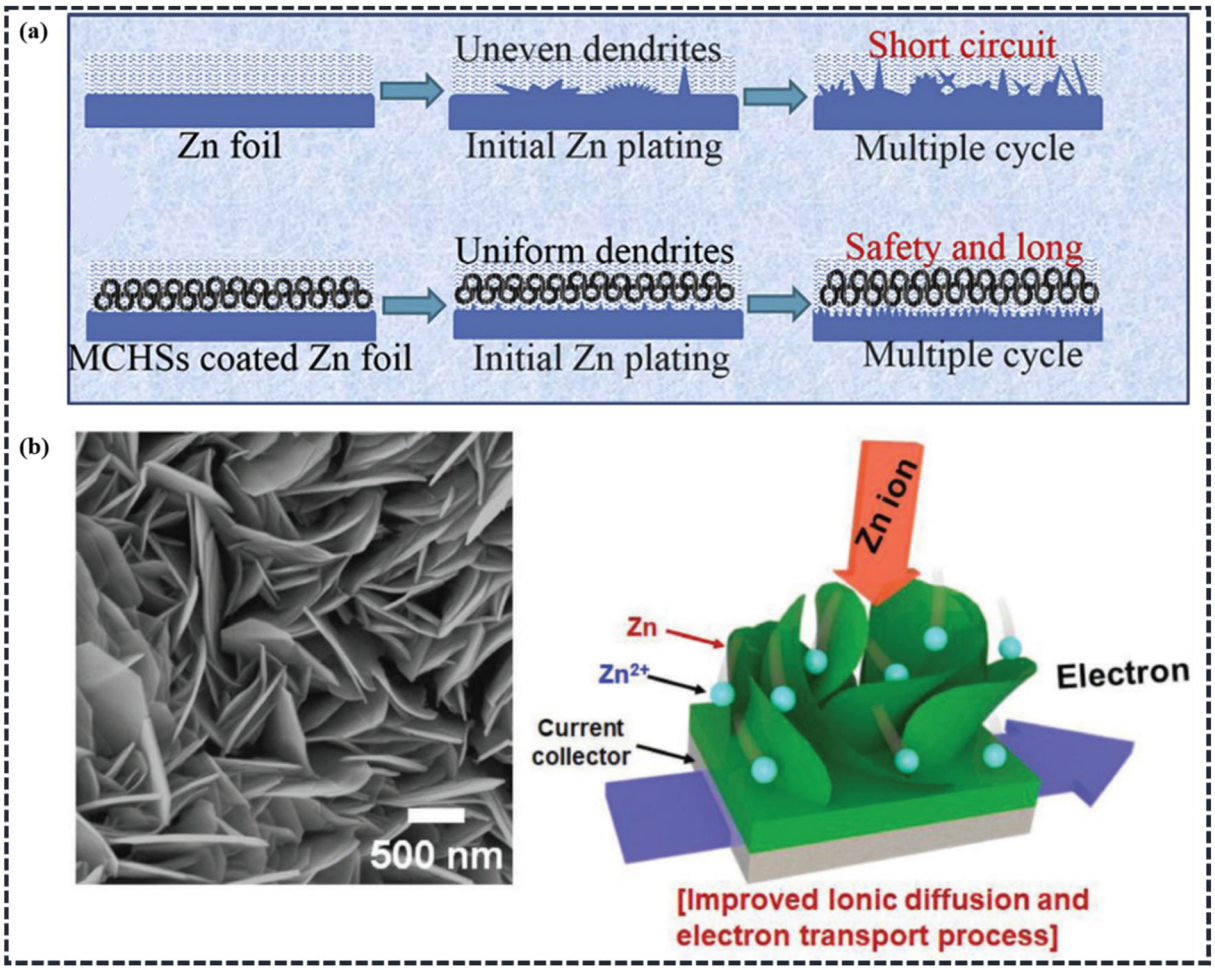

Fig. 9 (a) Schematics illustration showing the morphological progression for bare and MCHSs-coated Zn foils during Zn stripping/plating cycling (Reproduced from ref. 45 with permission from Elsevier). (b) FESEM image of 2D Zn, and schematic illustration of the 2D and hierarchically nanostructured Zn (2D-Zn) metal electrode for plating/stripping processes. (Reproduced from ref. 97 with permission from Wiley).

nanorods//activated carbon (AC) ZIHSC with $ZnSO_4$ aqueous electrolyte.[98] At the optimal mass ratio of AC to MnO_2, the ZIHSC exhibited a maximum specific capacity of 54.1 mA h g^{-1}, which translates to a maximum energy density of 34.8 W h kg^{-1}. This ZIHSC delivered a large power density of 3.3–13.0 kW kg^{-1} and can be charged/discharged quickly in approximately 2–17 seconds. To further improve the performance, Ren *et al.* used a simple electrodeposition technique to grow Na^+ pre-intercalated δ-MnO_2 nanoflakes ($Na_{0.11}MnO_2$) on three-dimensional graphene (3DG) for its usage as the cathode.[99] To evaluate the practical performance of the $Na_{0.11}MnO_2$/3DG electrode, a ZIHSC was constructed with the $Na_{0.11}MnO_2$/3DG cathode, AC anode, and an electrolyte composed of 2 M $ZnSO_4$ & 0.2 M $MnSO_4$. At a current density of 0.5 A g^{-1}, the ZIHSC produced a high specific capacitance of 165 F g^{-1} as calculated considering the total mass of active materials in the cathode and anode. Additionally, after 5000 charge/discharge cycles at 1 A g^{-1}, this ZIHSC exhibited remarkable cycling stability with a high capacitance retention of 83% and a coulombic efficiency of 99.5%. This device could deliver an impressive energy density of 74.3 W h kg^{-1} at a power density of 455.7 W kg^{-1} and a maximum power density of 9.6 kW kg^{-1} at 18 W h kg^{-1} energy density, demonstrating its strong power feature. Similarly, Ren *et al.* prepared Zn_xMnO_2-CNTs, which consisted of MnO_2 pre-intercalated with Zn^{2+} ions and doped with CNTs, as the battery-type cathode and activated carbon (AC) as the capacitor-type anode in an aqueous electrolyte containing both Zn^{2+} and Mn^{2+} ions.[33] A maximum energy density of 15.65 W h kg^{-1} was reached at a power density of 1800 W kg^{-1} with this ZIHSC. In addition, its cycling stability was excellent, as it exhibited a capacity retention of 97.5% after 6000 discharge/charge cycles. Similarly, Li *et al.* reported the N-MnO_2 nano-wall, which was *in situ* grown on flexible CC by electrodeposition.[44] As a result, the N-MnO_2 anode was assembled to an aqueous ZIHSC with an AC cathode, delivering a high energy density of 712.5 μW h cm^{-2} at a power density of 1000 μW cm^{-2} (1mA cm^{-2}) and superb cycling performance with 92.9% capacity retention after 25 000 charge/discharge cycles.

Vanadium-based oxides. Vanadium oxides and their derivatives are the most crucial materials being employed in the area of energy storage applications due to their abundant resources,

making them low-cost, and multiple oxidation states of vanadium (V) endowing rich pseudocapacitance. Recently, incredible research advancements with V-based compounds as zinc-ion battery (ZIB) electrode materials have been observed.[100,101] However, the application of V-based oxides as cathode materials in aqueous ZIHSCs is still scanty. Ma *et al.* designed and fabricated an AC//V_2O_5 ZIHSC with 2 M $ZnSO_4$ electrolyte, which exhibited maximum specific capacity and energy density of 57.4 mA h g^{-1} and 34.6 W h kg^{-1}, respectively, along with 97.3% capacity retention after 6000 charge/discharge cycles.[102] In another study, Li *et al.* demonstrated a ZIHMSC by using a vanadium pentoxide (V_2O_5) based cathode and a $Ti_3C_2T_x$ MXene-based anode in a PAM-$ZnSO_4$ hydrogel electrolyte.[85] This ZIHMS exhibited excellent electrochemical characteristics, including a high capacitance (129 mF cm^{-2} under 0.34 mA cm^{-2}), a high energy density (48.9 μW h cm^{-2} at 673 μW cm^{-2}), and good cycling stability with 77% capacitance retention over 10 000 cycles. Furthermore, Liang *et al.* synthesized lamellar structured $Ni_xV_2O_5{\cdot}nH_2O$ with *in situ* H_2O/Ni^{2+} intercalation and utilized it as the cathode material to assemble ZIHSCs with AC as the anode.[34] At a current density of 0.1 A g^{-1}, the ZIHSC delivered a specific capacity of 52 mA h g^{-1}, and an energy density of 27.2 W h kg^{-1} was achieved at a power density of 51.6 W kg^{-1}. Excellent cycling stability was observed, with the supercapacitor showing no signs of performance degradation even after 5000 cycles.

Titanium-based sulfide. Other than the previously mentioned Zn metal, Mn-based oxides, and V-based oxides, Ti-based sulfides, such as titanium disulfide (TiS_2), have also been used as the battery-type electrode materials in ZIHSCs. For example, Wang *et al.* constructed a ZIHSC utilizing a 2D layered TiS_2 battery-type anode and an active carbon capacitor-type cathode in 2 M $ZnSO_4$ electrolyte.[103] This ZIHSC delivered a high specific capacitance of 249 F g^{-1} at 0.2 A g^{-1}, a high energy density of 112 W h kg^{-1} at 180 W kg^{-1} and a good cycle life with a capacitance retention of 92% after 5000 cycles at 2 A g^{-1} current density.

Transition metal phosphide. Scientists have given close attention to transition-metal phosphides due to their tunable component structure, distinct physical/chemical properties, and abundance of active sites, which have significant advantages over transition-metal oxides and hydroxides in energy storage and conversion fields. For instance, Guo *et al.* synthesized double-transition-metal phosphide $Co_xNi_{2-x}P$/rGO composites by a typical hydrothermal method.[104] This was followed by the successful execution of the electrodeposition method in a two-electrode system to synthesize a Zn-ion-activated CoNiP/rGO (Zn@CoNiP/rGO) anode material with Zn nanosheets vertically placed into the surface of the CoNiP/rGO composites. Consequently, when paired with a biomass-derived PC cathode in 2 M $ZnSO_4$ electrolyte, the as-assembled ZIHSCs demonstrated a high specific capacitance of 356.6 F g^{-1} at 0.5 A g^{-1}, an exceptional energy density of 143.14 W h kg^{-1}, and an outstanding cycling stability of 92.2% capacitance retention after 10 000 cycles at 7.5 A g^{-1}.

4.3 Electrolytes for ZIHSCs

The electrolyte, which determines the reversibility of Zn stripping/plating efficiency as well as controls the corrosion and dendritic development of the Zn anode, is a vital component of ZIHSCs in addition to the electrode materials and hence, significantly affects the electrochemical performance of ZIHSCs. Many traits, including high ionic conductivity, low viscosity, a large operating potential window, an appropriate ionic size for fast intercalation/deintercalation, and high thermal stability to achieve a wide working temperature range, are crucial for selecting an efficient electrolyte. However, for ZIHSCs, only a few electrolyte systems have so far been able to satisfy these requirements. In the following subsections, a complete description of the effects of aqueous electrolytes, non-aqueous electrolytes, and certain novel kinds of electrolytes on the electrochemical performance of ZIHSCs is provided.[12,105]

4.3.1 Aqueous electrolytes. Aqueous electrolytes are inexpensive, easy to handle, safer, and more environmentally friendly as compared to non-aqueous electrolytes, and have an extremely high ionic conductivity. High ionic mobility in an aqueous medium guarantees smaller resistance which is crucial in enhancing the rate performance of the device. The most popular aqueous electrolytes for ZIHSCs are $ZnSO_4$, $Zn(CF_3SO_3)_2$, $Zn(CH_3COO)_2$, $Zn(NO_3)_2$, $ZnCl_2$, and $Zn(ClO_4)_2$. Wu *et al.* first examined how electrolyte concentration and different anions in the electrolyte impacted the electrochemical performance of aqueous ZIHSCs.[106] The average coulombic efficiency (CE) in 1 M (1 M means 1-mole solute dissolved in per kilogram of deionized water) $Zn(CF_3SO_3)_2$, $Zn(CH_3COO)_2$, $ZnCl_2$, and $ZnSO_4$ electrolytes for the first 50 cycles was 90.4, 90.0, 86.8, and 82.7%, respectively. While 1 M $Zn(NO_3)_2$ displayed the lowest CE (~0%), and the $Zn(CF_3SO_3)_2$ electrolyte has high reversibility for Zn stripping/plating with the highest average CE observed. In addition, the effects of electrolyte concentration on the average CE were carefully analyzed, and the average CE of ZIHSCs was found to improve with the increase in electrolyte concentration, irrespective of the type of electrolyte used. The average CE with $Zn(CF_3SO_3)_2$ electrolyte reached the maximum when the concentration was above 3 M and then remained invariant with the further increase in electrolyte concentration. The average CEs for 3 M and 4 M $Zn(CF_3SO_3)_2$ aqueous electrolytes were calculated to be 96.8 and 97.0%, respectively, for the first 50 cycles and further increased to 98.4 and 98.9%, respectively, during the next 1000 cycles, indicating high reversibility of Zn plating and stripping processes in this solution. By contrast, the average CEs for 3 M $ZnSO_4$ and $ZnCl_2$ electrolytes were calculated to be only 89.8 and 91.3%, respectively, for the first 50 cycles. Finally, a ZIHSC with 3 M $Zn(CF_3SO_3)_2$ electrolyte, porous carbon derived from a chemically activated graphene (aMEGO) cathode, and Zn foil anode was developed. This ZIHSC provided a high energy density of 106.3 W h kg^{-1} and a high power density of 31.4 kW kg^{-1} with an outstanding 93% capacity retention after

80 000 cycles. Moreover, Huang *et al.* employed three different aqueous electrolytes, $Zn(CH_3COO)_2$, $ZnCl_2$, and $ZnSO_4$, to study how different anion carriers affected the electrochemical behavior of titanium nitride-based zinc ion hybrid supercapacitors (Zn-TiN ZIHSCs).[89] Electrochemical performance comparison of Zn-TiN ZIHSCs with various anion carriers revealed that the type of anion plays an important role in determining the capacitance as well as self-discharge properties of Zn-TiN ZIHSCs (Fig. 10a–c). DFT calculations further revealed that the SO_4^{2-} anions have the lowest adsorption energy (−6.3942 eV) on the Zn-TiN electrode as compared to acetate (AC^-) and Cl^- ions, and hence, the Zn-TiN electrode exhibited the best electrochemical performance and most superior anti-self-discharge ability in $ZnSO_4$ solution. For instance, the ZIHSC with $ZnSO_4$ electrolyte delivered a high capacitance of 489.8 F g^{-1} at a current density of 0.2 A g^{-1} and 314.5 F g^{-1} after 10 000 cycles at a current density of 1 A g^{-1}.

4.3.2 Non-aqueous electrolytes. Non-aqueous electrolytes, such as organic electrolytes and ionic liquid electrolytes, have recently attracted significant attention in the field of ZIHSCs because they offer a wider operating potential window than aqueous electrolytes do, resulting in a higher energy density.[8,107] However, issues regarding poor electronic conductivity resulting in poor rate performance and high flammability causing severe safety concerns need to be addressed before their widespread use in practical ZIHISCs. Wang *et al.* fabricated ZIHSCs utilizing bio-carbon derived porous material as the cathode, Zn foil as the anode, and with two different electrolytes; one contained 1 M $Zn(CF_3SO_3)_2$ dissolved in a 1 : 1 (v/v) mixture of dimethoxyethane (DME) and 1,3-dioxolane (DOL), and the other one used 1 M $Zn(CF_3SO_3)_2$ dissolved in acetonitrile (AN).[108] They optimized the electrolytes and observed that the ZIHSC with 1 M $Zn(CF_3SO_3)_2$ dissolved in acetonitrile exhibited superior electrochemical performance. They argued that owing to the high dielectric constant (38.8) and dipole moment (3.92 D), the AN could offer high conductivity and hence good capacitance retention at higher currents. For instance, the ZIHSC with AN offered a high discharge capacitance of 170 F g^{-1} at 0.1 A g^{-1} along with a good rate capability of ∼85% at 2 A g^{-1}. Moreover, it also achieved a high energy density of 52.7 W h kg^{-1} at a power density of 1725 W kg^{-1} (based on the mass of active materials) and demonstrated a 91% capacitance retention over 20 000 cycles observed at 2 A g^{-1}. Similarly, Zhou *et al.* designed ZIHSCs using a functionalized carbon nanosponge cathode and Zn anode, however, with two different electrolytes: (1) $Zn(CF_3SO_3)_2$ in ionic liquid (IL, $EMIMCF_3SO_3$) and (2) $Zn(CF_3SO_3)_2$ in acetonitrile (AN).[109] The totally packed cell with IL delivered a superior volumetric energy density of 54.3 W h L^{-1} within a wide operating voltage of 2.4 V. However, an ultrahigh power density of 17.7 kW L^{-1} with a good energy density of 18.8 W h L^{-1}, and bettered rate capability were achieved by changing the IL to AN which can be credited to the lower viscosity of AN. The full charge/discharge of the ZIHSC with AN took only 11 seconds. More importantly, the ZIHSC with AN demonstrated excellent stability, with no change in capacitance for well over 60 000 cycles. In another report, Pappu *et al.* fabricated the first ZIHSC with an exfoliated graphene oxide (EGO) incorporated $NiCo_2O_4$ composite material as a positive electrode and commercial YP-50F carbon as a negative electrode in 1 M $TEABF_4$ acetonitrile organic electrolyte.[110] The device demonstrated a specific capacity of 28.3 mA h g^{-1} (equivalent to 37.4 F g^{-1}) at 1 A g^{-1} with 80.2% capacity retention at 10 A g^{-1}, and an energy-power combination of 37.8 W h kg^{-1} and 1350 W kg^{-1}, respectively. This device retained 98% of its initial capacitance after 10 000 GCD cycles measured at 2 A g^{-1}.

4.3.3 New types of electrolytes. Now, to address the problems like electrolyte leakage and a small voltage window with aqueous electrolytes, and severe safety concerns with non-aqueous electrolytes, and to further boost the energy storage performance of ZIHSCs, a number of new electrolytes have been designed and garnered significant research as well as technological interests as next-generation electrolytes. In this regard, suitable gel electrolytes that are safe, stable, flexible, possess good ionic conductivity, and are easy to process are highly required to improve the practical feasibility of ZIHSCs for next-generation device applications.[111–113] Yang *et al.* prepared a flexible ZIHSC using a solid-state cellulose hydrogel electrolyte containing highly concentrated $ZnCl_2$.[114] This ZIHSC demonstrated high durability at a low temperature of −20 °C. The device also achieved a very high specific capacity of 193 mA h g^{-1} at 0.5 A g^{-1}, an excellent energy density of 192 W h kg^{-1} at a power density of 499 W kg^{-1}, and 94.7%

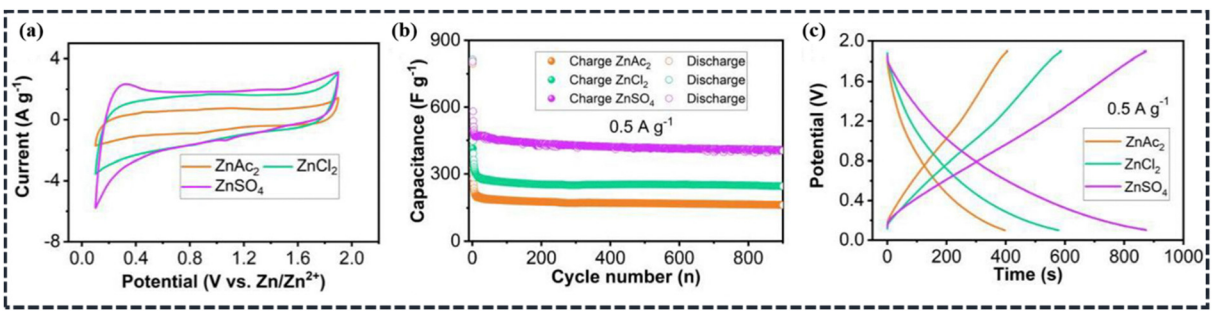

Fig. 10 (a) Comparison of CV curves at a scan rate of 10 mV s^{-1} for the TiN electrode tested in different electrolytes including $Zn(CH_3COO)_2$, $ZnCl_2$, and $ZnSO_4$, (b) cycling performance and (c) corresponding GCD curves of the Zn-TiN capacitor in different electrolyte media. (Reproduced from ref. 89 with permission from Wiley).

capacity retention after 5000 cycles indicating excellent potential with gel-based electrolytes.

Similarly, Han *et al.* assembled a solid-state ZIHSC with Zn foil and activated carbon electrodes and a zwitterionic natural polymer hydrogel as the electrolyte.[115] This hydrogel exhibited great mechanical strength and flexibility. Within a wide and stable voltage window of 2.4 V, this ZIHSC delivered an exceptionally high energy density of 286.6 W h kg^{-1} at a power density of 220 W kg^{-1} and exceptional capacity retention of 95.4% after 2000 cycles at 2 A g^{-1} current density. Likewise, Han *et al.* prepared a novel redox bromide-ion additive hydrogel electrolyte (SA-Zn-Br, Fig. 11a) to improve the performance of flexible ZIHSCs by including extra faradaic contribution from the $3Br^-/Br_3^-$ redox couple in the hydrogel electrolyte.[116] This flexible ZIHSC operated within a wide potential window of 0–2.6 V and resulted in an astounding energy density of 605 W h kg^{-1} at a power density of 1848 W kg^{-1}, along with a capacity retention of 87.7% after 5000 cycles. Such extraordinary performance of the ZIHSCs could be credited to the SA-Zn-Br hydrogel electrolyte, which can facilitate Zn-ion migration for uniform nucleation on the anode surface, and also mitigate corrosion by inhibiting water oxidation to allow highly reversible Zn plating/stripping reactions. Liu *et al.* reported a gel electrolyte based on the poly(vinyl alcohol) (PVA)/Zn/ethylene glycol system which is anti-freezing, easy to handle, non-toxic, and safe (Fig. 11b).[117] The anti-freezing ZIHSC fabricated with the optimum anti-freezing gel electrolyte membrane displayed exceptional electrochemical behaviors with a high potential window of 0–2 V and a high specific capacitance of 247.7 F g^{-1} at room temperature. Moreover, the

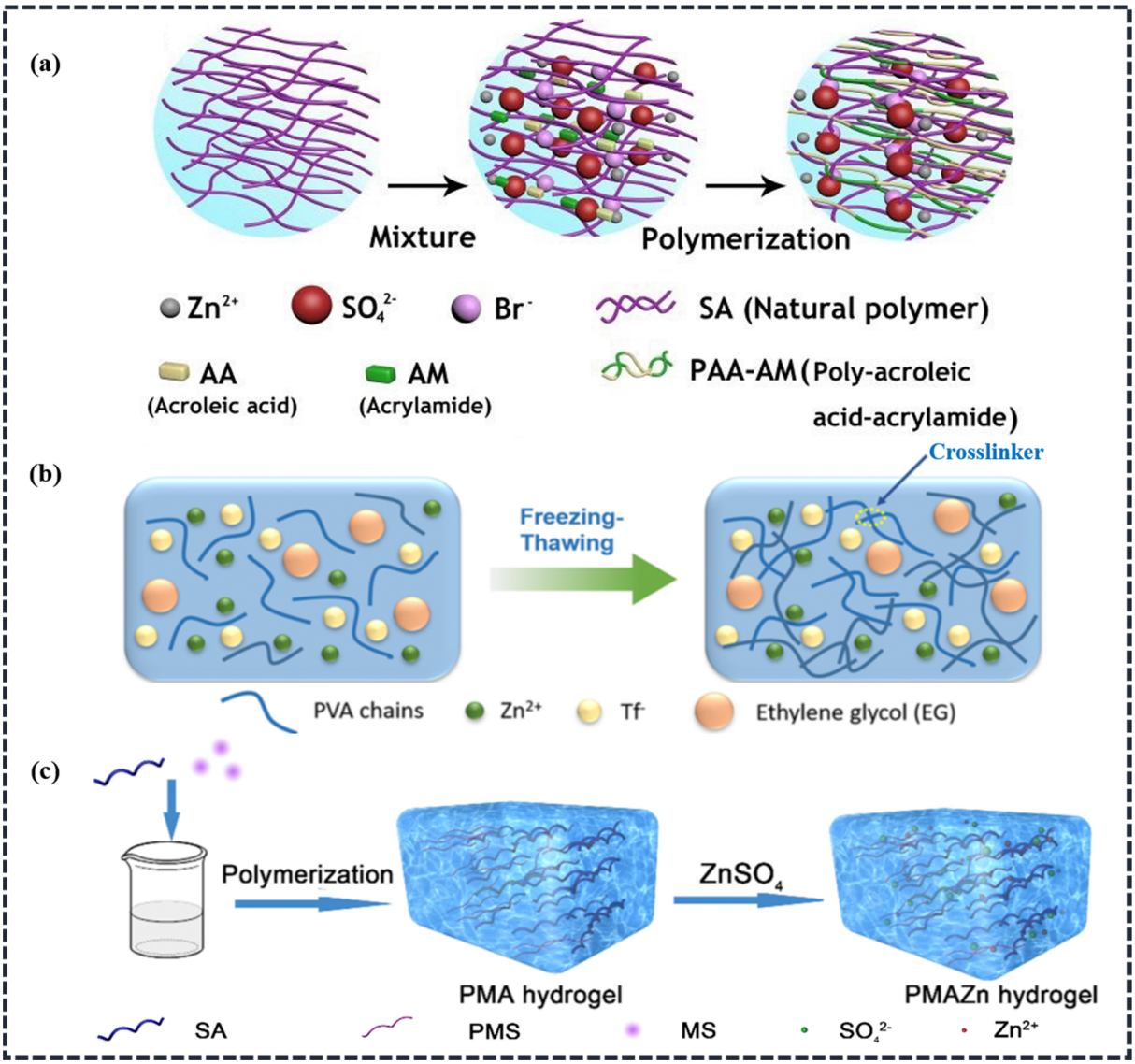

Fig. 11 Schematic illustration of (a) the SA-Zn-Br synthesis route (reproduced from ref. 116 with permission from Royal Society of Chemistry), (b) preparation of the anti-freezing gel electrolyte membrane (reproduced from ref. 117 with permission from American Chemical Society), and (c) PMA-Zn hydrogel synthesis process (reproduced from ref. 118 with permission from Elsevier).

Table 1 Summary of configurations and electrochemical performances of various ZIHSCs reported in this study

Sl. no.	Cathode//anode	Electrolyte	Potential window (V)	Capacity (mA h g^{-1})	Energy density (W h kg^{-1})	Power density (W kg^{-1})	Cycling stability	Ref.
1	AC//Zn foil	2 M $ZnSO_4$	0.2–1.8	121 (0.1 A g^{-1})	84	14.9	91% after 10 000 cycles	26
2	N, S-PCD//Zn foil	2 M $ZnSO_4$	0.2–1.8	133.4 (0.2 A g^{-1})	106.7	16	97.1% after 100 000 cycles	29
3	NPG//Zn foil	1 M $ZnSO_4$	0–1.8	105.1 (0.5 A g^{-1})	94.6	449.9	82% after 15 000 cycles	32
4	$Ni_xV_2O_5{\cdot}nH_2O$//AC	$ZnSO_4$	0.3–1.6	52 (0.1 A g^{-1})	27.2	51.6	100% after 5000 cycles	34
5	Zn-MnO_2//AC	2 M $ZnSO_4$	0–2	157.2 (0.2 A g^{-1})	157.2	—	80.2% after 30 000 cycles	35
6	MCHSs//Zn foil	2 M $ZnSO_4$	0.2–1.8	174.7 (0.1 A g^{-1})	129.3	266.4	100% after 10 000 cycles	45
7	WC-6ZnN-12U//Zn foil	2 M $ZnSO_4$	0.2–1.8	111 (0.1 A g^{-1})	109.5	255	92.7% after 50 000 cycles	47
8	PCM//Zn foil	2 M $Zn(CF_3SO_3)_2$	0–1.9	113.3 (0.1 A g^{-1})	64.9	35	136% after 5000 cycles	49
9	CSAC//Zn	3 M $Zn(ClO_4)_2$	0–1.8	141.5 (0.1 A g^{-1})	190.3	89	—	50
10	MSCP//Zn foil	2 M $ZnSO_4$	0–1.8	68.2 (0.68 A g^{-1})	36.5	376.6	85.4% after 10 000 cycles	51
11	PCNF//Zn foil	1 M $ZnSO_4$	0.1–1.7	108.2 (0.5 A g^{-1})	142.2	400.3	90% after 10 000 cycles	52
12	HPAC//Zn foil	3 M $Zn(CF_3SO_3)_2$	0.01–1.8	231 (0.5 A g^{-1})	77.5	11 400	70% after 18 000 cycles	53
13	P&B-AC//Zn foil	2 M $ZnSO_4$	0.2–1.8	169.4 (0.5 A g^{-1})	169.4	500	88% after 30 000 cycles	54
14	PHCA//Zn foil	2 M $ZnSO_4$	0.1–1.8	143.7 (1 A g^{-1})	129.3	1000	92% after 10 000 cycles	55
15	NSPCK//Zn foil	1 M $Zn(CF_3SO_3)_2$	0–1.8	136.3 (0.1 A g^{-1})	122.6	58.3	99.5% after 15 000 cycles	56
16	S-3DPC//Zn foil	2 M $ZnSO_4$	0.2–1.8	203.3 (0.2 A g^{-1})	162.6	160	96.8% after 18 000 cycles	57
17	PSC-A*x*//Zn foil	1 M $Zn(CF_3SO_3)_2$	0.2–1.8	183.7 (0.2 A g^{-1})	147	136.1	92.2% after 10 000 cycles	66
18	GRPC-A13//Zn foil	2 M $ZnSO_4$	0.2–1.8	177 (0.5 A g^{-1})	116	800	50% after 270 000 cycles	67
19	LDC//Zn foil	Gelatin/$ZnSO_4$	0.2–1.8	116.8 (0.5 A g^{-1})	86.8	429.6	81.3% after 6500 cycles	71
20	CNPK//Zn foil	1 M $ZnSO_4$	0.2–1.8	103.2 (0.1 A g^{-1})	81.1	65	100% after 10 000 cycles	72
21	N,P-OLC//Zn foil	2 M $ZnSO_4$	0.2–1.8	184.5 (0.5 A g^{-1})	149.5	350	—	73
22	EG/PANI//POP-TAPP-NTCA	2 M $ZnSO_4$	0.1–1.5	66.8	48	65	90% after 1100 cycles	78
23	$RuO_2{\cdot}H_2O$//Zn foil	2 M $Zn(CF_3SO_3)_2$	0.4–1.6	122 (0.1 A g^{-1})	119	90	87.5% after 10 000 cycles	94
24	MnO_2//AC	2 M $Zn(CF_3SO_3)_2$	0–2	46.4 (0.1 A g^{-1})	29.5	60	93.4% after 5000 cycles	98
25	V_2O_5//AC	$ZnSO_4$	0–2	57.4 (0.1 A g^{-1})	34.6	—	97.3% after 6000 cycles	102

ZIHSC exhibited extraordinary electrochemical performance and cycling stability even after 30 000 cycles at −20 °C. Meanwhile, Chen *et al.* prepared a hydrogel electrolyte by the zwitterionic monomer [2-(methacryloyloxy)ethyl]dimethyl-(3-sulfopropyl) (MS) and sodium alginate (SA), as schematically presented in Fig. 11c.[118] The zwitterionic double-network hydrogel offered good mechanical strength and also alleviated the issue of zinc dendrite growth. When operated within a wide potential window of 0–2.4 V, the hydrogel electrolyte-based ZIHSC delivered a high specific capacity of 159.4 mA h g^{-1} and a good energy-power combination of 88.5 W h kg^{-1}–172.3 W kg^{-1}, respectively.

A brief summary of different capacitor-type, battery-type electrode materials, and electrolytes used in ZIHSCs along with their performances are presented in Table 1.

5. Recent developments in the field of ZIHSCs

While the current generation ZIHSCs have garnered significant research and technological attention due to their safety, reliability, and performance, they cannot be considered suitable for next-generation miniaturized, lightweight, flexible, and wearable device applications. Additionally, considering the global shift towards renewable energy resources, solar-powered energy storage devices are promising for green energy harvesting and storage. Therefore, further innovations in the design and development of ZIHSCs are inevitable and highly coveted. In this regard, the development of flexible ZIHSCs, micro ZIHSCs, and photo rechargeable ZIHSCs, has been undertaken to achieve some additional unique features with ZIHSCs like miniaturization, flexibility, wearability, and photo rechargeability. By leveraging ever-evolving technological breakthroughs, ZIHSCs with new and multiple functionalities are being explored to expand their application prospects. A few such recent developments are summarized in the following subsections.

5.1 Flexible ZIHSCs

Due to their unique qualities, such as high flexibility, excellent stability, and durability under extremely strained conditions, flexible Zn-ion batteries (f-ZIBs) have drawn much interest from researchers and manufacturers of alternative energy storage systems. In this regard, the discovery of ZIHSCs further increased the interest in flexible ZIHSCs (f-ZIHSCs) because of their attractive properties, such as their ultra-long cycle lifespan, low cost, excellent safety, and little environmental impact. Electrodes and gel electrolytes (GEs) significantly affect the performance of f-ZIHSCs since they must be mechanically flexible and show a high degree of stability and durability under various stress conditions.[28]

Huang *et al.* assembled an f-ZIHSC using a PVA-based gel electrolyte, polydopamine-coated porous carbon cloth (PDA@PCC) as a flexible cathode, and Zn@CC as the anode.[119] The CC was preactivated *via* an air calcination process to facilitate the loading of PDA and Zn^{2+} ion absorption. Interestingly, an areal capacity of 0.92 mA h cm^{-2} was achieved with this f-ZIHSC, which corresponds to an areal capacitance of 1948 mF cm^{-2}. Furthermore, the f-ZIHSC also displayed a maximum energy density of 9.7 mW h cm^{-3} at a power density of 14 mW cm^{-3} along with a 92% capacitance retention after 500 cycles. The device demonstrated good flexibility and durability when made to undergo some extreme condition tests, such as cutting and sewing tests.

Similarly, Ni *et al.* realized an f-ZIHSC with poly(vinyl alcohol) (PVA)/$Zn(CF_3SO_3)_2$ aqueous gel as the electrolyte, a MWCNTs-RGO-Zn hybrid fiber anode, and a MWCNTs-RGO hybrid fiber cathode.[120] The energy density of this f-ZIHSC was 13.1 mW h cm^{-3}, and the power density was 1433.2 mW cm^{-3}, demonstrating excellent electrochemical performance. Capacitance was still retained at over 80% after 10 000 GCD cycles, and the coulombic efficiency was quite high throughout the cycle duration. To further check the feasibility of practical application in flexible devices, the flexibility of f-ZIHSC was studied in detail under different bending conditions. Fig. 12a shows the digital photograph of the device demonstrating the excellent flexibility of the f-ZIHSC. Fig. 12b and c shows the CV and GCD curves at specific scan rates and current densities, respectively, of the f-ZIHSC with bending angles varying from 0° to 150°. After analyzing the data, it can be realized that the f-ZIHSC retained 87.8% of the original specific capacitance and 77.6% of the original energy density when the f-ZIHSC was bent from 0 to 150° (Fig. 12d and e). The nature of the Nyquist plots (Fig. 12f) of the f-ZIHSC remains almost identical during the whole bending process, which indicates excellent stability of the electrodes and the gel electrolyte. The cycling performance of the f-ZIHSC was studied for 4000 GCD cycles at a current density of 1.5924 A cm^{-3} under a bending angle of 150°, during which the device maintained specific capacitance and coulombic efficiency well above 90%, as shown in Fig. 12g. Further in Fig. 12h, the application potential of the f-ZIHSC in a practical scenario was investigated where the power delivery by the f-ZIHSC was found to be invariant under different bending conditions. Interestingly, Han *et al.* developed an f-ZIHSC using zwitterionic natural polymer hydrogel electrolyte along with Zn foil and activated carbon electrodes. The bending durability of the prepared device was tested extensively utilizing different parameters, including the bending angle (θ), the bending radius of curvature (R), and the length of the device (L), as demonstrated in Fig. 13aI–aIII.[115]

As per Fig. 13a-II, the f-ZIHSC could maintain capacities between 100% and 92.4% when the device was bent from 0 to 180° thanks to the excellent flexibility and electrochemical stability of the electrodes as well as the hydrogel electrolyte. Similarly, when tested over multiple bending cycles for a fixed θ of 90°, R = 0.15 cm and L = 2 cm, the capacity retentions of the

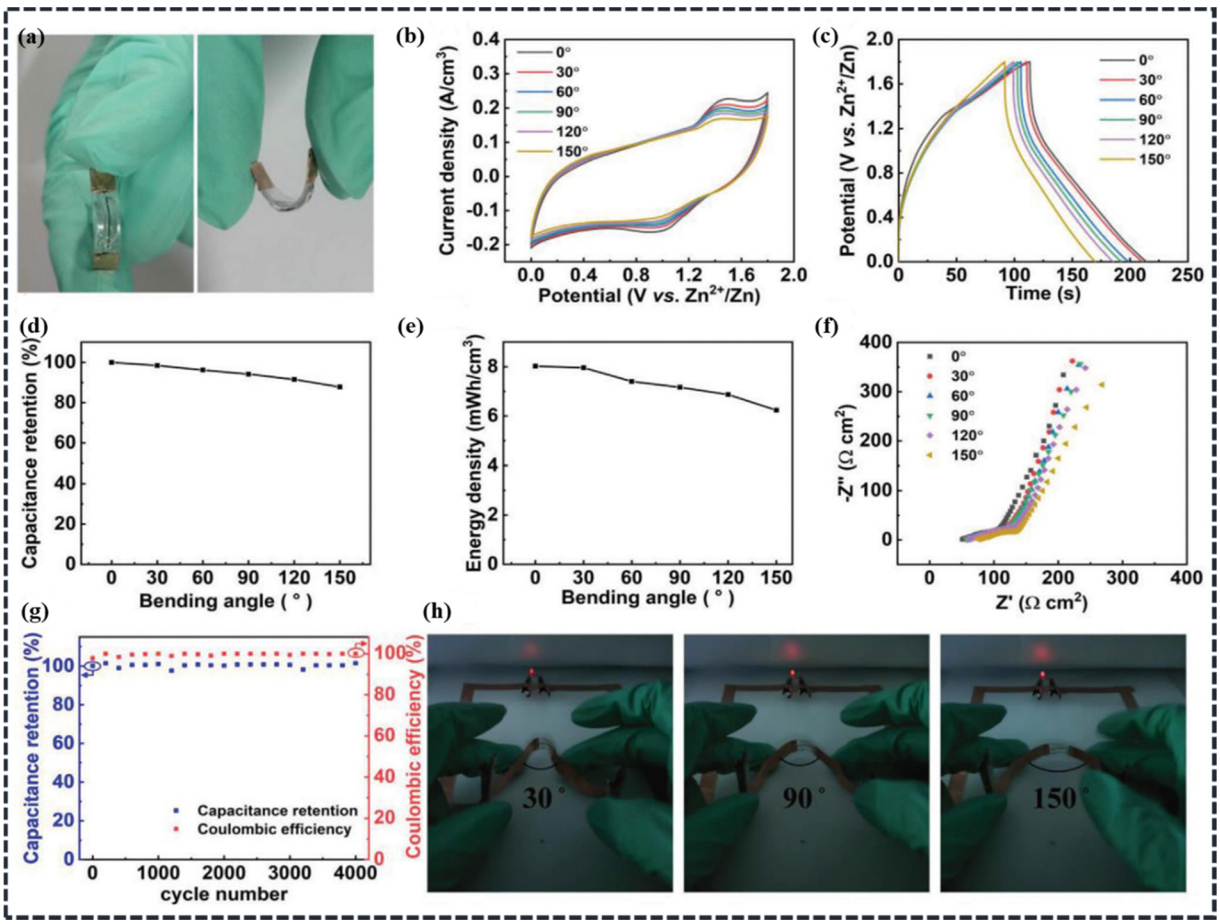

Fig. 12 Flexibility tests of the f-ZIHSC: (a) digital photograph of the f-ZIHSC in the bent state, (b) CV curves, (c) GCD curves, (d) capacitance retention, (e) energy density and (f) Nyquist plots of the f-ZIHSC with different bending angles, (g) capacitance retention and coulombic efficiency *versus* cycle number of the f-ZHSC under the bending angle of 150°, and (h) digital photographs of an LED bulb powered by the f-ZIHSC under various bending angles. (Reproduced from ref. 120 with permission from Wiley).

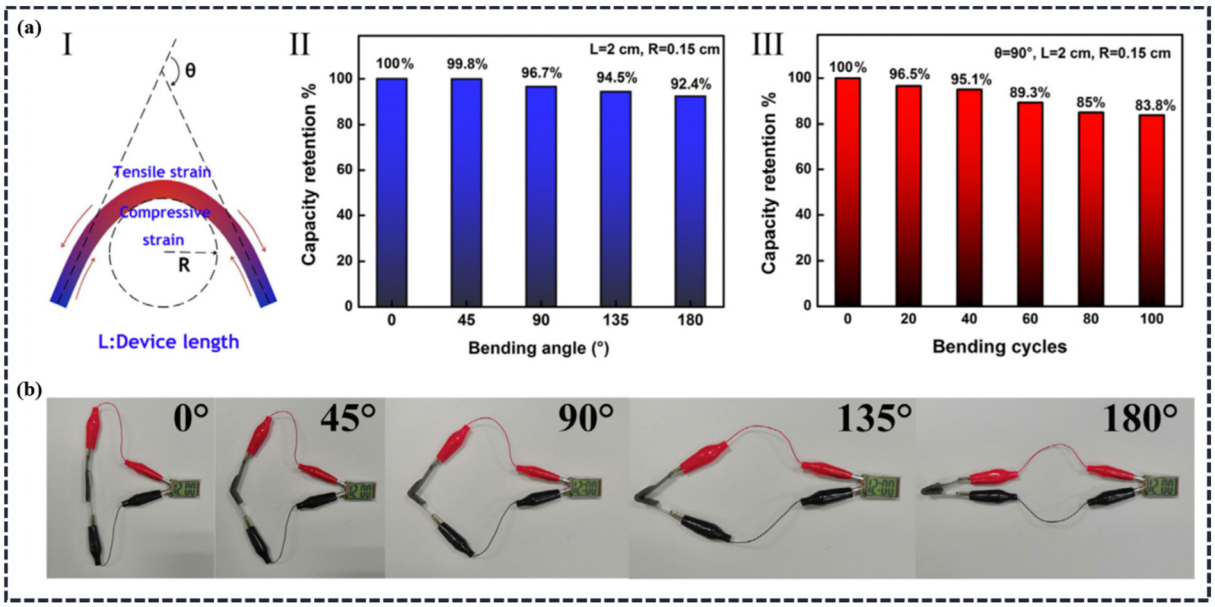

Fig. 13 (a-I) Diagram showing the structure of the device and three crucial parameters (bending angle θ, bending radius R (= 0.15 cm), and fixed length L (= 2 cm)) used to show the bending states of the f-ZIHSC. (a-II) Capacity retentions of the f-ZIHSC at different bending angles (varied from 0 to 180°). (a-III) Capacity retentions of the f-ZIHSC upon 100 bending cycles at a fixed bending angle of 90°. (b) Digital images of an electrical watch powered by the f-ZIHSC at different bending states. (Reproduced from ref. 115 with permission from Elsevier).

f-ZIHSC varied between 100% and 83.8% during 100 bending cycles (Fig. 13a-III), again indicating superior stability. Moreover, the f-ZIHSC could effectively power an electrical timepiece at various bending angles, as shown in Fig. 13b.

5.2 Zinc ion micro supercapacitors (ZIMSCs)

Fast development in miniaturization, mobility, and highly integrated electronic technology has generated significant interest in micro-sized energy storage devices with outstanding electrochemical performance. For instance, Li *et al.* proposed a facile laser writing approach to fabricate a patterned $Ti_3C_2T_x$-based cathode for a Zn ion micro supercapacitor (ZIMSC). The Zn anode was directly obtained *via* an electrodeposition process, and PVA/$ZnCl_2$ gel was used as the electrolyte for assembling the ZIMSC, having a thickness of 0.851 μm.[121] The assembled ZIMSC after annealing treatment delivered the maximum areal capacitance of 72.02 mF cm^{-2} (662.53 F cm^{-3}) at a scan rate of 10 mV s^{-1}, provided a power density of 0.50 mW cm^{-2} at an areal energy density of 0.02 mW h cm^{-2} with superior rate stability and exhibited 80% capacitance retention even after 50 000 charge/discharge cycles. Cao *et al.* assembled a symmetrical ZIMSC with electrodes based on interdigital MXene/bacterial cellulose fiber (BCF) hybrid film prepared *via* the laser-cutting technique and neutral 2 M $Zn(CF_3SO_3)_2$/polyacrylamide (PAM) hydrogel electrolyte.[122] Schematics of the synthesis of interlayer expanded MXene/BCF hybrid films, laser cutting technique, and microdevice assembly are shown in Fig. 14a. The device demonstrated a high areal energy density of 34.0 μW h cm^{-2}. This study offers a straightforward and efficient method for realizing symmetric ZIMSCs with a high areal energy density, good rate capability, and cycling stability by increasing bivalent Zn^{2+} diffusion through expanded ion transport channels between few-layered MXene sheets and simultaneously suppressing the hydrogen/oxygen evolution kinetics to allow the symmetric ZIMSC to achieve a higher working voltage.

Li *et al.* used $Ti_3C_2T_x$ MXene as a capacitor-type anode and vanadium pentoxide (V_2O_5) as a battery-type cathode to design a ZIMSC (Fig. 14b).[85] The electrolyte was $ZnSO_4$-dissolved polyacrylamide (PAM) hydrogel. The flexible ZIMSC demonstrated excellent electrochemical characteristics, including high capacitance (129 mF cm^{-2} at 0.34 mA cm^{-2}), an energy-power combination of 48.9 μW h cm^{-2} and 673 μW cm^{-2}, respectively, and 77% capacitance retention after 10 000 cycles. Similarly, Mao *et al.* demonstrated a degradable ZIMSC based on the MXene/$ZnCl_2$ anode and MnO_2-MWCNTs cathode assembled with $MnSO_4$/$ZnSO_4$ gel electrolyte.[86] This microdevice delivered a high areal capacitance of 64.49 F cm^{-2} at 0.10 mA cm^{-2} and over 83% capacitance retention after 8000 charge–discharge cycles. Furthermore, when made to undergo bending tests, the microdevice demonstrated excellent flexibility at different bending angles (0–180°).

5.3 Photo-rechargeable ZIHSCs

With the rapid development in energy technologies, many sustainable energy resources have been intensively investigated, including wind, solar, ocean, biomass, geothermal, hydropower, *etc.* The direct storage of solar energy is complicated and even unrealistic. Generally, solar energy is first converted into other forms of energy and then stored. By far, there have been some usual methods for converting and storing solar energy, such as solar-to-thermal, solar-to-biomass,

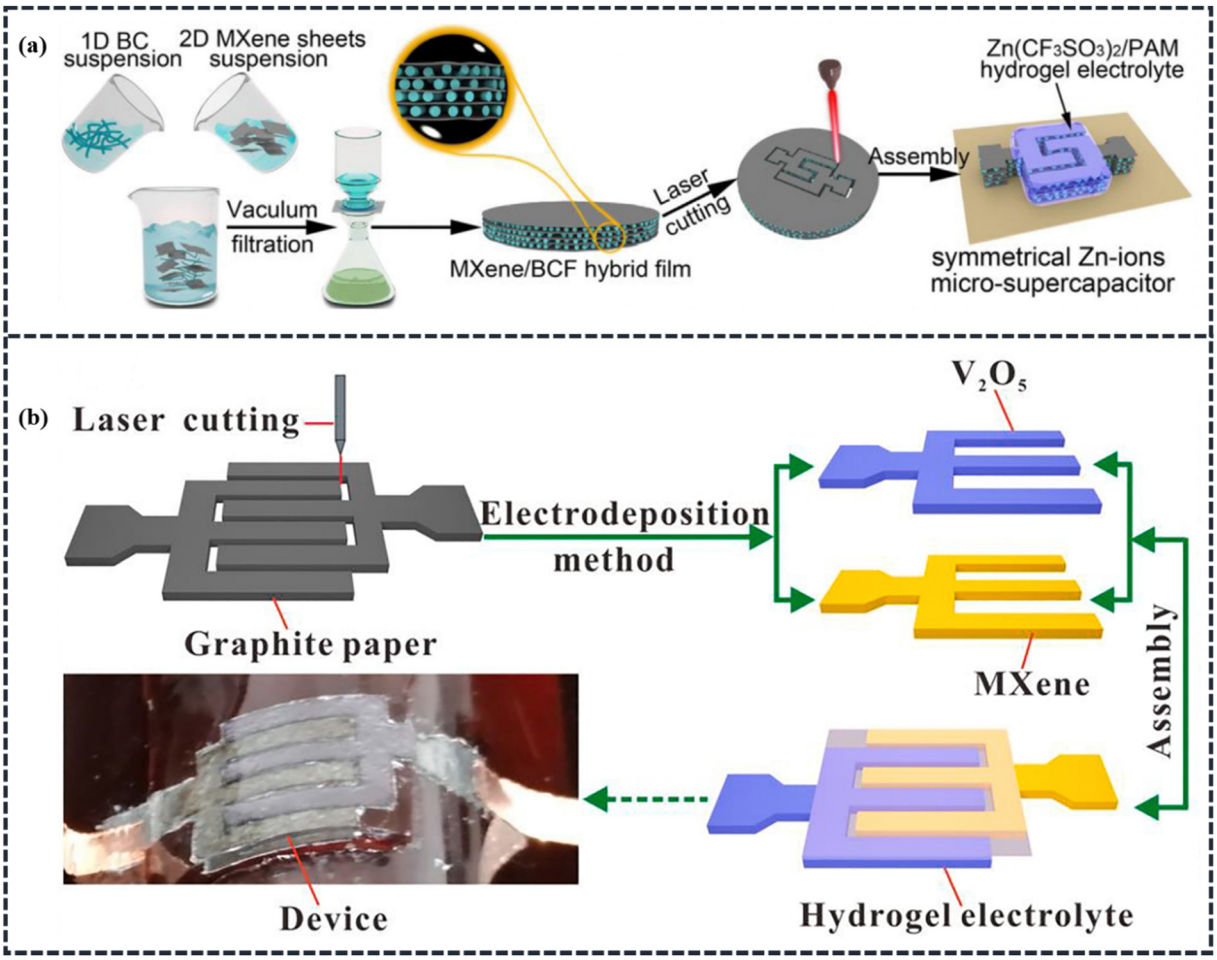

Fig. 14 (a) Illustration of the complete fabrication process of the symmetrical aqueous Zn-ion-based MSCs with MXene/BCF hybrid film electrodes. (Reproduced from ref. 122 with permission from Elsevier). (b) The preparation and assembly process of the ZIMSC based on the $Ti_3C_2T_x$ MXene anode, V_2O_5 cathode, and $ZnSO_4$/PAM hydrogel electrolyte. (Reproduced from ref. 85 with permission from Elsevier).

solar-to-chemical, and solar-to-electrochemical. Amongst others, solar-to-electrochemical energy conversion and storage technology is found to be the more facile and low-cost procedure.[123,124]

For the first time, Boruah *et al.* designed a photoactive 2D g-C_3N_4 cathode (as shown in Fig. 15a) and Zn metal foil anode-based photo-rechargeable zinc-ion capacitor (Photo-ZIC, Fig. 15b).[125] In this Photo-ZIC, 2D g-C_3N_4 serves as a light-harvesting material that can charge directly under visible light irradiation without the need for any additional photovoltaic devices, allowing it to simultaneously collect solar energy and store it in the form of charge. The operation of the Photo-ZIC can be described as follows: in the presence of light, photo-generated electrons move from g-C_3N_4 to fluorine-doped tin oxide (FTO) and gather on the surface of the Zn anode through the external circuit, where they facilitate the electrolyte's Zn^{2+} ions to deposit. Meanwhile, the anions (such as SO_4^{2-}) that are attracted by the photogenerated free holes on g-C_3N_4 may gather and adsorb on the surface of the g-C_3N_4 cathode (Fig. 15b). Fig. 15c compares the CV responses at 50 mV s^{-1} under dark and illumination conditions where a significant increase in current density could be observed under illumination indicating storage of the photogenerated charge carriers. The as-fabricated photo-ZIC device has demonstrated a photo-charging voltage response of about 850 mV, a photo-rechargeable specific capacitance of 11 377 mF g^{-1}, photocharge energy densities of 0.7 W h kg^{-1}, and light conversion efficiency of about 0.01%. Furthermore, the device could also retain almost 90% of the capacitance after 1000 cycles indicating good cycling stability of the electrodes and the device. The same group fabricated photo-rechargeable ZIC using AC as the cathode and one-dimensional Ag@V_2O_5 nanofibers as the photoanode, as demonstrated schematically in Fig. 15d.[126] The photoanode was prepared by drop casting a mixture of V_2O_5 and Ag nanowires on an FTO coated glass substrate. Zn strips were used to make contact between the FTO and coin cell for efficient transport of photogenerated holes. The bandgap of V_2O_5 is adequate to respond to visible light irradiation, and its distinctive layered structure allows reversible intercalation and deintercalation of Zn^{2+} ions. As in Fig. 15e, a comparison of the CV response at 50 mV s^{-1} under dark and illumination conditions indicates capacity enhancement under illumination. However, in contrast to the previously reported photo-ZIC

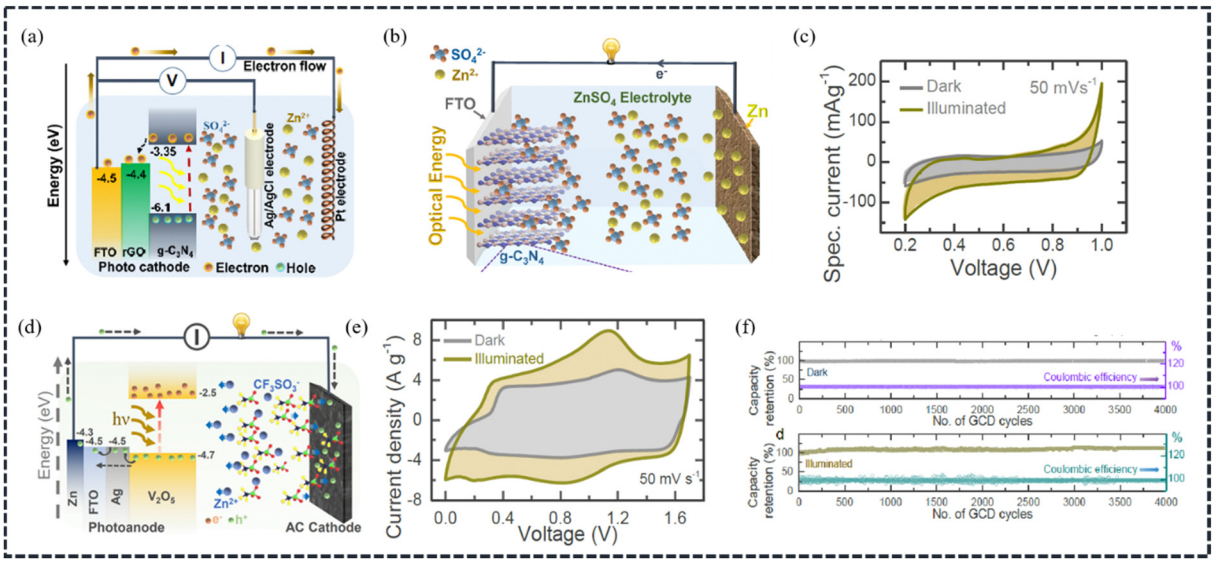

Fig. 15 (a) Schematic representation of the design of the g-C_3N_4@rGO/FTO photoelectrode in a three-electrode setup, (b) schematic diagram of the photo-ZIC with a 2D g-C_3N_4 cathode, Zn anode, and $ZnSO_4$ aqueous electrolyte, (c) CVs collected for the photo-ZIC in the dark and under illuminated conditions. (Reproduced from ref. 125 with permission from American Chemical Society). (d) Schematic representation of photo-ZIC based on a Ag@V_2O_5 photoanode and AC cathode, (e) its CV curves at scan rates of 50 mV s^{-1}, and (f) its cycling performance at 200 mA g^{-1} under dark and illuminated conditions. (Reproduced from ref. 126 with permission from American Chemical Society).

(ref. 125), this one achieved a much better photoconversion efficiency of 0.05%, a much higher photocharge energy density of 4.8 W h kg^{-1}, and photocharge capacitance (138 F g^{-1}). These results represent 5-, 7-, and 12-fold improvements in conversion efficiency, photocharge energy density, and capacitance, respectively, as compared to the 2D g-C_3N_4-based photo-ZIC. Additionally, under both dark and light settings, the Ag@V_2O_5 photo-ZIC device provided an exceptional energy density of 53 W h kg^{-1} and good capacitance retention of 99% after 4000 cycles (Fig. 15f). The findings of this study also indicate that Ag nanowires outperform carbon-based materials including SCNTs and MCNTs in speeding up the transmission of the photogenerated holes in V_2O_5 and improving visible light absorption by acting as light scattering centers.

A summary of the electrochemical performances of flexible ZIHSCs, micro ZIHSCs, and photorechargeable ZIHSCs are presented in Table 2.

6. Summary and future perspective

From the Ragone plot in Fig. 1, comparing energy-power densities of different current-generation energy storage devices, it could be understood that ZIHSCs have potential as safe and inexpensive alternatives to LIBs and hence are highly appropriate for next-generation energy applications. While the research on ZIHSCs has made significant developments over the last couple of years, their widespread applications are still in their infancy as there are several challenges to overcome first. As the main components of any electrochemical energy storage device, electrodes (capacitor-type and battery-type) and electrolytes substantially impact the ZIHSC's performance, including capacity, energy/power density, and cycle life. In this section, we summarize some challenges, possible solutions, and opportunities with ZIHSCs based on state-of-the-art studies as well as our understanding, knowledge, and consideration.

Capacitor type electrode

For the ZIHSCs, the capacitor-type electrodes are generally based on capacitive materials such as AC, PC, heteroatom-doped carbon, pseudocapacitive MXene, conducting polymers, and a few transition metal oxides. Generally, carbon materials have several advantages over others, like ease of processing, low cost, excellent physical/chemical stability, and high SSA, which could boost the ion's adsorption/desorption processes and reduce the cost of the device fabrication as well. However, the low specific capacitance of carbon-electrode materials, which limits the energy density, is the primary concern. Various strategies are implemented to improve the specific capacity of carbon materials as follows.

(a) Tuning electrodes' microstructure. It is well known that increasing specific surface area and tuning the porosity of electrode materials greatly impacts the electrochemical performance of energy storage devices, including ZIHSCs. The active surface area may be increased by tuning the dimensionality of the electrode materials, which increases the proportion of electrode surface area exposed to the electrolyte. As a result, unique 3D electrode microstructures with interconnected pores have offered a more accessible region for electrolyte diffusion as well as easy paths for fast charge movement, resulting in greater electrical contact. Nevertheless, shortened diffusion paths caused by interconnected pores accelerate ion transfer during redox reactions, which is crucial for the pseudocapacitive electrode materials exhibiting great performance.[5,127] Moreover, macropores act as ion reservoirs to provide enough

Table 2 Summary of the configurations and performance parameters for different flexible ZIHSCs, micro ZIHSCs, and photorechargeable ZIHSCs reported in this study

Flexible ZIHSCs

Sl. no.	Cathode//anode	Electrolyte	Potential window	Capacity	Energy density	Power density	Cycling stability	Ref.
1	AC//Zn foil	Cellulose hydrogel/$ZnCl_2$	0–2 V	193 mA h g^{-1} (0.5 A g^{-1})	192 W h kg^{-1}	499 W kg^{-1}	94.7% after 5000 cycles	114
2	AC//Zn foil	SA-Zn hydrogel	0–2.4	260.5 mA h g^{-1} (0.2 A g^{-1})	286.6 W h kg^{-1}	220 W kg^{-1}	85.9% after 10 000 cycles	115
3	AC//Zn foil	SA-Zn-Br hydrogel	0–2.6	654.8 mA h g^{-1} (2 A g^{-1})	605 W h kg^{-1}	1848 W kg^{-1}	87.7% after 5000 cycles	116
4	Graphene//Zn	Gel electrolyte	0–2	247.7 F g^{-1} (0.2 A g^{-1})	137.2 W h kg^{-1}	199.7 W kg^{-1}	73.7% after 50 000 cycles	117
5	AC//Zn foil	PMA/Zn hydrogel	0–2.4	159.4 mA h g^{-1} (0.5 A g^{-1})	88.56 W h kg^{-1}	172.3 W kg^{-1}	74.5% after 10 000 cycles	118
6	PDA@PCC//Zn	PVA gel	0.1–1.8	0.92 mA h cm^{-2}	9.7 mW h cm^{-3}	14 mW cm^{-3}	92% after 500 cycles	119
7	MWCNTs-RGO// MWCNTs-RGO-Zn	PVA/$Zn(CF_3SO_3)_2$	0–1.8	41.2 F cm^{-3}	13.1 mW h cm^{-3}	200 mW cm^{-3}	80.8% after 10 000 cycles	120
Zinc Ion Micro Supercapacitors (ZIMSCs)								
1	AC//Zn	$ZnSO_4$	0.5–1.5	259.4 F g^{-1} (0.05 A g^{-1})	115.4 μW h cm^{-2} at 0.16 mA cm^{-2}	0.16 mW cm^{-2}	100% after 10 000 cycles	63
2	Poly(3,3′-DHB)/AC//Zn	$ZnSO_4$	0.5–1.5	1.1 F cm^{-2} (0.5 mA cm^{-2})	152 μW h cm^{-2}	300 μW cm^{-2}	80% after 3000 cycles	76
3	MnO_2-MWCNTs// MXene/$ZnCl_2$	$MnSO_4$/$ZnSO_4$ gel	0–1.8	64.49 F cm^{-2} (0.10 mA cm^{-2})		—	83.1% after 8000 cycles	86
4	$Ti_3C_2T_x$//Zn	PVA/$ZnCl_2$ gel	0–1.4	72.02 mF cm^{-2} (10 mV s^{-1})	0.02 mW h cm^{-2}	0.50 mW cm^{-2}	80% after 50 000 cycles	121
5	MXene/BCF//MXene/BCF	2 M $Zn(CF_3SO_3)_2$/ PAM hydrogel	0–1.2	178.6 mF cm^{-2}	34.0 μW h cm^{-2}	—	72.3% after 3000 cycles	122

Photo-rechargeable ZIHSCs

	Cathode//anode	Electrolyte	Photo-charging conversion efficiency	Photo-charged specific capacitances	Photo-charged energy density	Photo-charged power density	Cycling stability	Ref.
1	g-C_3N_4@rGO/FTO//Zn foil	2 M $ZnSO_4$	0.01%	11.4 F g^{-1}	668 mW h kg^{-1}	1625 mW kg^{-1}	90% after 1000 cycles	125
2	AC//Ag@V_2O_5	3 M $Zn(CF_3SO_3)_2$	0.05%	138 F g^{-1}	53.13 W h kg^{-1}	36.74 W kg^{-1}	100% after 4000 cycles	126

supply of ions at higher current rates, mesopores facilitate electrolyte ion diffusion, and micropores improve ion adsorption/desorption. Therefore, it is crucial to design and create a 3D hierarchical porous structure to enhance ion adsorption/desorption kinetics and fast ion migration for enhanced energy storage. For instance, Gittins *et al.* prepared MOF samples with 'flake-like' particles and a pore network comprising many short pores, which displayed superior capacitive performance compared to samples with either 'rod-like' or strongly agglomerated particles.[128]

(b) Heteroatom doping. Electronic structure and surface characteristics of carbon materials can be controlled effectively by heteroatom doping. These heteroatoms not only help in tuning the electrical characteristics of the host carbon but also serve as reaction centers to facilitate chemical adsorption and desorption of ions and hence, add extra pseudocapacitance. In addition, the heteroatom doping technique could also be employed to improve the ionic diffusion capability and wettability of AC and hence could result in an enhancement of the energy storage performance of ZIHSCs.

(c) Design of carbon-based composites. Pseudocapacitive materials, although they deliver higher specific capacitance than carbon materials, are poorer in rate capability and cycling stability, and hence reduce the overall performance of ZIHSCs preventing their practical use. This suggests that combining carbon with different kinds of pseudocapacitive materials to achieve a larger capacity, better rate capability and cycle life, and sometimes a broader working voltage window as compared to pristine carbons, would be an attractive choice for high-performance capacitor-type electrode materials. In addition, exploration of some novel capacitor-type electrode materials, including pristine TMOs, composites of TMOs with MXenes and conducting polymers, transition metal sulfides/nitrides, and binary metal hydroxides, would open up more possibilities for the advancement of ZIHSCs.

Battery type electrode

Generally, metallic Zn, V- and Mn-based oxides are often employed as battery-type electrode materials in ZIHSCs. The most popular battery-type electrode material for ZIHSCs is the commercial Zn foil. Unfortunately, it comes with some inherent problems that cannot be avoided, including dendrite formation, corrosion, and the HER, which makes it very difficult to achieve excellent electrochemical performance. Inhibition of dendrite growth and increase in the ion's diffusion/transport capacity can however be achieved by constructing 3D nanostructured Zn electrodes, which would guarantee uniformly distributed electric fields owing to enhanced electrochemically active surface area. In the future, cost-effective 3D printing technology would be a viable option for realizing 3D Zn electrodes on a large scale.

Additionally, surface coating technology is another powerful method for suppressing Zn dendrite formation and corrosion. It prevents the metal's direct contact with the electrolyte, significantly improving the anode's reversibility and durability. Therefore, modifying the 3D Zn microstructure *via* surface coating technology is a potential research area to realize a highly stable, reversible, and dendrite-free Zn anode. Furthermore, key difficulties with the intercalation-type anodes (V- and Mn-based oxides) are their poor capacities and cycling performance owing to the phase or structural changes they undergo during the charge/discharge cycles. However, such problems can be overcome efficiently by using advanced carbon coating techniques, preparing hydrated intercalation anodes, and by pre-intercalation of alkali metal ions.

Electrolyte

As the electrolyte is one of the crucial components of any electrochemical energy storage device, the following requirements with the electrolytes need to be satisfied to improve the performance and ensure the safety of ZIHSCs: (a) the electrolyte must have a wide operating voltage window to achieve high energy density; (b) should have a high ionic conductivity to enhance the power density and reduce the internal resistance; (c) it should be inexpensive, and environmentally friendly; (d) it should be structurally and electrochemically stable for achieving long cycle life; and most importantly, (e) the size of the ions in the electrolyte must be compatible with the pore size of the electrode material for easy and fast diffusion.

All of the aforementioned characteristics are met by aqueous electrolytes, with the only exception of a large working voltage window, which prevents the ZIHSCs from achieving a high level of energy density. ZIHSCs may, however, attain a high energy density when using non-aqueous electrolytes (organic or ionic liquid electrolytes), allowing high operating voltage. But, several issues related to their safety, high cost, poor ionic conductivity, high viscosity, and large ionic radii have not yet been adequately addressed and need further study. Further, extensive studies on gel electrolytes for energy and power-dense ZIHSCs are highly coveted considering their broad working voltage window, safety, flexibility, and wide working temperature range. Such studies would also address the problems regarding weak ion conductivity and small electrode/electrolyte contact area of the gel electrolytes.

New strategies for device design and development

Although ZIHSCs have made some remarkable advancements in recent years, the design and development of new, multifunctional ZIHSC devices are still in their infancy. There is still much work to be conducted in regard to the design of new electrolytes and novel electrode materials with good flexibility, high mechanical strength, and unique properties that would incorporate self-healing traits and stretchability in flexible ZIHSCs device. Making a new composite electrode based on a lightweight, highly conductive material with a 3D porous design would be the best approach in this regard. A robust approach to improve the electrochemical performance of flexible-ZIHSCs is the development of gel electrolytes with high ionic conductivity. More facile and effective ways to build microelectrodes and microdevices are also being explored. These devices might get benefit from the recently developed 3D printing technology, which would also make it easier to integrate them with other microelectronic systems on a chip.

The use of solid or semi-solid gel electrolytes is always beneficial to avoid leakage-related issues with liquid electrolytes. However, the limited ionic conductivity of solid electrolytes limits the power density of microdevices. Therefore, apart from developing solid electrolytes with good ionic conductivity and anti-freezing benefits, the development of proper encapsulating materials and techniques are also required to realize micro ZIHSCs with a high degree of flexibility and reliability. In the case of photo-rechargeable ZICs, although several remarkable advances have been achieved, there is still scope for improvements in areas including their cost-effectiveness and poor photo-conversion efficiency.

Author contributions

Himanshu Gupta: writing – original draft, writing – review & editing. Manoj Kumar: supervision, writing – review & editing. Debasish Sarkar: resources, conceptualization, supervision, project administration, writing – review & editing, Prashanth Menezes: supervision, writing – review & editing.

Conflicts of interest

The authors declare no competing financial interest.

Acknowledgements

H. G. acknowledges Ministry of Education (MoE), Government of India, for the senior research fellowship. D. S. acknowledges financial support from the ISRO-RAC-S MNIT Jaipur through project RAC-S/PRO/21-22/02 and UGC-DAE CSR Indore through project CRS/2021-22/01/442. P. W. M. acknowledges funding by the German Federal Ministry of Education and Research in the framework of the project Catlab (03EW0015A/B).

References

1 C. Liu, F. Li, L.-P. Ma and H.-M. Cheng, *Adv. Mater.*, 2010, **22**, E28–E62.
2 A. Noori, M. F. El-Kady, M. S. Rahmanifar, R. B. Kaner and M. F. Mousavi, *Chem. Soc. Rev.*, 2019, **48**, 1272–1341.
3 P. Aggarwal, D. Sarkar, K. Awasthi and P. W. Menezes, *Coord. Chem. Rev.*, 2022, **452**, 214289.
4 R. Sun, M. Dou, Z. Chen, R. Wang, X. Zheng, Y. Zhang, C. Zhou and P. W. Menezes, *Battery Energy*, 2023, **2**, 20220064.
5 A. Kumar, H. K. Rathore, D. Sarkar and A. Shukla, *Electrochem. Sci. Adv.*, 2022, **2**, e2100187.
6 D. Selvakumaran, A. Pan, S. Liang and G. Cao, *J. Mater. Chem. A*, 2019, **7**, 18209–18236.
7 S. K. Sharma, G. Sharma, A. Gaur, A. Arya, F. S. Mirsafi, R. Abolhassani, H.-G. Rubahn, J.-S. Yu and Y. K. Mishra, *Energy Adv.*, 2022, **1**, 457–510.
8 Y. Shao, M. F. El-Kady, J. Sun, Y. Li, Q. Zhang, M. Zhu, H. Wang, B. Dunn and R. B. Kaner, *Chem. Rev.*, 2018, **118**, 9233–9280.
9 P. Simon and Y. Gogotsi, *Nat. Mater.*, 2008, **7**, 845–854.
10 P. Simon and Y. Gogotsi, *Nat. Mater.*, 2020, **19**, 1151–1163.
11 Y. Gogotsi and P. Simon, *Science*, 2011, **334**, 917–918.
12 C. Zhong, Y. Deng, W. Hu, J. Qiao, L. Zhang and J. Zhang, *Chem. Soc. Rev.*, 2015, **44**, 7484–7539.
13 H. Wang, W. Ye, Y. Yang, Y. Zhong and Y. Hu, *Nano Energy*, 2021, **85**, 105942.
14 X. Lu, Y. Zeng, M. Yu, T. Zhai, C. Liang, S. Xie, M.-S. Balogun and Y. Tong, *Adv. Mater.*, 2014, **26**, 3148–3155.
15 D. Sarkar, D. Das, S. Nagarajan and D. Mitlin, *Sustainable Energy Fuels*, 2022, **6**, 3582–3590.
16 D. Das, D. Sarkar, S. Nagarajan and D. Mitlin, *Chem. Commun.*, 2020, **56**, 14889–14892.
17 A. Amiri, E. N. Swart and A. A. Polycarpou, *Renew. Sustainable Energy Rev.*, 2021, **148**, 111288.
18 Z. Wang, M. Zhang, W. Ma, J. Zhu and W. Song, *Small*, 2021, **17**, 2100219.
19 X. Gong, J. Chen and P. S. Lee, *Batteries Supercaps*, 2021, **4**, 1529–1546.
20 Z. Li, Y. An, S. Dong, C. Chen, L. Wu, Y. Sun and X. Zhang, *Energy Stor. Mater.*, 2020, **31**, 252–266.
21 D. Zhang, L. Li, J. Deng, S. Guo, H. Pang, J. Lu, D. Xia and X. Ji, *Nanoscale*, 2021, **13**, 11004–11016.
22 Q. Liu, H. Zhang, J. Xie, X. Liu and X. Lu, *Carbon Energy*, 2020, **2**, 521–539.
23 J. Yin, W. Zhang, N. A. Alhebshi, N. Salah and H. N. Alshareef, *Adv. Energy Mater.*, 2021, **11**, 2100201.
24 H. Tang, J. Yao and Y. Zhu, *Adv. Energy Mater.*, 2021, **11**, 2003994.
25 X. Deng, J. Li, Z. Shan, J. Sha, L. Ma and N. Zhao, *J. Mater. Chem. A*, 2020, **8**, 11617–11625.
26 L. Dong, X. Ma, Y. Li, L. Zhao, W. Liu, J. Cheng, C. Xu, B. Li, Q.-H. Yang and F. Kang, *Energy Stor. Mater.*, 2018, **13**, 96–102.
27 J. Yin, W. Zhang, W. Wang, N. A. Alhebshi, N. Salah and H. N. Alshareef, *Adv. Energy Mater.*, 2020, **10**, 2001705.
28 M. S. Javed, S. Asim, T. Najam, M. Khalid, I. Hussain, A. Ahmad, M. A. Assiri and W. Han, *Carbon Energy*, 2023, **5**, e271.
29 Y. Yang, D. Chen, H. Wang, P. Ye, Z. Ping, J. Ning, Y. Zhong and Y. Hu, *Chem. Eng. J.*, 2022, **431**, 133250.
30 Y. Peng, Y. Bai, C. Liu, S. Cao, Q. Kong and H. Pang, *Coord. Chem. Rev.*, 2022, **466**, 214602.
31 Q. Li, M. Liu, F. Huang, X. Zuo, X. Wei, S. Li and H. Zhang, *Chem. Eng. J.*, 2022, **437**, 135494.
32 Y. Zhao, H. Hao, T. Song, X. Wang, C. Li and W. Li, *J. Power Sources*, 2022, **521**, 230941.
33 D. Ren, X. Li, X. Zhao, B. Liu, Z. Yang, J. He, T. Li and P. Pan, *Appl. Energy*, 2022, **324**, 119730.
34 X. Liang, J. Li, X. Yang, L. Wang, X. Li and W. Lü, *J. Energy Storage*, 2022, **56**, 105947.
35 S. He, Z. Mo, C. Shuai, W. Liu, R. Yue, G. Liu, H. Pei, Y. Chen, N. Liu and R. Guo, *Appl. Surf. Sci.*, 2022, **577**, 151904.

36 Y. Dahiya, M. Hariram, M. Kumar, A. Jain and D. Sarkar, *Coord. Chem. Rev.*, 2022, **451**, 214265.
37 H. Jiang, D. Yuan, D. Huang, B. Lin, J. Li, P. Guo and Y. Wang, *Appl. Surf. Sci.*, 2022, **585**, 152695.
38 Y. Xu, X. Chen, C. Huang, Y. Zhou, B. Fan, Y. Li, A. Hu, Q. Tang and K. Huang, *J. Power Sources*, 2021, **488**, 229426.
39 Y. Wei, X. Chen, G. Gao, D. Shen, H. Rong and Q. Liu, *Ionics*, 2022, **28**, 3477–3488.
40 T. Xiong, Y. Shen, W. S. V. Lee and J. Xue, *Nano Mater. Sci.*, 2020, **2**, 159–163.
41 C. R. K. Rao and D. C. Trivedi, *Coord. Chem. Rev.*, 2005, **249**, 613–631.
42 S. Wu, S. Zhang, Y. Chu, Z. Hu and J. Luo, *Adv. Funct. Mater.*, 2021, **31**, 2107397.
43 J. Zhang, Q. Yao, S. Tang, C. Yang, Q. Liu, L. Zang and J. Qiu, *J. Mater. Sci.*, 2022, **57**, 19936–19945.
44 K. Li, J. Li, L. Wang, X. Li, X. Yang and W. Lü, *J. Alloys Compd.*, 2022, **928**, 167153.
45 P. Liu, W. Liu, Y. Huang, P. Li, J. Yan and K. Liu, *Energy Storage Mater.*, 2020, **25**, 858–865.
46 S. Chen, L. Ma, K. Zhang, M. Kamruzzaman, C. Zhi and J. A. Zapien, *J. Mater. Chem. A*, 2019, **7**, 7784–7790.
47 G. Lou, G. Pei, Y. Wu, Y. Lu, Y. Wu, X. Zhu, Y. Pang, Z. Shen, Q. Wu, S. Fu and H. Chen, *Chem. Eng. J.*, 2021, **413**, 127502.
48 G. Zhao, D. Yu, H. Zhang, F. Sun, J. Li, L. Zhu, L. Sun, M. Yu, F. Besenbacher and Y. Sun, *Nano Energy*, 2020, **67**, 104219.
49 X. Zhang, E. Cao, Y. Tian, M. Zhang, X. Liu, Z. Lei, Z. Zhao, P. Cui, Q. Ling and R. Xie, *Carbon Resour. Convers.*, 2022, **5**, 193–199.
50 G. Yang, J. Huang, X. Wan, Y. Zhu, B. Liu, J. Wang, P. Hiralal, O. Fontaine, Y. Guo and H. Zhou, *Nano Energy*, 2021, **90**, 106500.
51 S. Zeng, X. Shi, D. Zheng, C. Yao, F. Wang, W. Xu and X. Lu, *Mater. Res. Bull.*, 2021, **135**, 111134.
52 Z. Pan, Z. Lu, L. Xu and D. Wang, *Appl. Surf. Sci.*, 2020, **510**, 145384.
53 Z. Zhou, X. Zhou, M. Zhang, S. Mu, Q. Liu and Y. Tang, *Small*, 2020, **16**, 2003174.
54 Y.-G. Lee and G.-H. An, *ACS Appl. Mater. Interfaces*, 2020, **12**, 41342–41349.
55 H. Fan, S. Zhou, Q. Chen, G. Gao, Q. Ban, Z. Xu, F. He, G. Hu and X. Hu, *J. Power Sources*, 2021, **493**, 229687.
56 F. Wei, H. Zhang, J. Wang, J. Zhuang and Y. Lv, *J. Alloys Compd.*, 2022, **907**, 164536.
57 D. Wang, S. Wang and Z. Lu, *Int. J. Energy Res.*, 2021, **45**, 2498–2510.
58 Y. Zhai, Y. Dou, D. Zhao, P. F. Fulvio, R. T. Mayes and S. Dai, *Adv. Mater.*, 2011, **23**, 4828–4850.
59 L. L. Zhang and X. S. Zhao, *Chem. Soc. Rev.*, 2009, **38**, 2520–2531.
60 J. Liu, S. Ahmed, T. Wang and S. Song, *Chem. Eng. J.*, 2023, **451**, 138512.
61 P. Pattananuwat, R. Pornprasertsuk, J. Qin and S. Prasertkaew, *RSC Adv.*, 2021, **11**, 35205–35214.
62 Z. Fan, J. Yan, T. Wei, L. Zhi, G. Ning, T. Li and F. Wei, *Adv. Funct. Mater.*, 2011, **21**, 2366–2375.
63 P. Zhang, Y. Li, G. Wang, F. Wang, S. Yang, F. Zhu, X. Zhuang, O. G. Schmidt and X. Feng, *Adv. Mater.*, 2019, **31**, 1806005.
64 H. Liu, X. Liu, W. Li, X. Guo, Y. Wang, G. Wang and D. Zhao, *Adv. Energy Mater.*, 2017, **7**, 1700283.
65 G. Singh, K. S. Lakhi, S. Sil, S. V. Bhosale, I. Kim, K. Albahily and A. Vinu, *Carbon*, 2019, **148**, 164–186.
66 Z. Li, D. Chen, Y. An, C. Chen, L. Wu, Z. Chen, Y. Sun and X. Zhang, *Energy Stor. Mater.*, 2020, **28**, 307–314.
67 L. Yao, J. Jiang, H. Peng, H. Yang, S. Liu, X. Wen, P. Cai, Y. Zou, H. Zhang, F. Xu, L. Sun and X. Lu, *J. Energy Storage*, 2023, **58**, 106378.
68 S. Ghosh, S. Barg, S. M. Jeong and K. Ostrikov, *Adv. Energy Mater.*, 2020, **10**, 2001239.
69 Y. Li, G. Wang, T. Wei, Z. Fan and P. Yan, *Nano Energy*, 2016, **19**, 165–175.
70 J. Ding, Z. Li, K. Cui, S. Boyer, D. Karpuzov and D. Mitlin, *Nano Energy*, 2016, **23**, 129–137.
71 Y. Lu, Z. Li, Z. Bai, H. Mi, C. Ji, H. Pang, C. Yu and J. Qiu, *Nano Energy*, 2019, **66**, 104132.
72 H. Zhang, Z. Chen, Y. Zhang, Z. Ma, Y. Zhang, L. Bai and L. Sun, *J. Mater. Chem. A*, 2021, **9**, 16565–16574.
73 H. Wang, Q. Chen, P. Xiao and L. Cao, *ACS Appl. Mater. Interfaces*, 2022, **14**, 9013–9023.
74 Q. Meng, K. Cai, Y. Chen and L. Chen, *Nano Energy*, 2017, **36**, 268–285.
75 G. He, Y. Liu, D. E. Gray and J. Othon, *Compos. Commun.*, 2021, **27**, 100882.
76 N. Wang, T. Xin, Y. Zhao, Q. Li, M. Hu and J. Liu, *ACS Sustainable Chem. Eng.*, 2019, **7**, 14195–14202.
77 T. Xin, Y. Wang, N. Wang, Y. Zhao, H. Li, Z. Zhang and J. Liu, *J. Mater. Chem. A*, 2019, **7**, 23076–23083.
78 F.-Z. Cui, Z. Liu, D.-L. Ma, L. Liu, T. Huang, P. Zhang, D. Tan, F. Wang, G.-F. Jiang and Y. Wu, *Chem. Eng. J.*, 2021, **405**, 127038.
79 D. T. Tung, H. M. Nguyet, N. T. Dung, H. T. Dung, N. T. Yen, N. B. Thanh, P. N. Hong, P. Van Hoi, N. Van Quynh, P. N. Minh and L. T. Lu, *J. Electron. Mater.*, 2021, **50**, 4407–4414.
80 K. S. Kumar, N. Choudhary, Y. Jung and J. Thomas, *ACS Energy Lett.*, 2018, **3**, 482–495.
81 S.-K. Hwang, S. J. Patil, N. R. Chodankar, Y. S. Huh and Y.-K. Han, *Chem. Eng. J.*, 2022, **427**, 131854.
82 M. R. Lukatskaya, S. Kota, Z. Lin, M.-Q. Zhao, N. Shpigel, M. D. Levi, J. Halim, P.-L. Taberna, M. W. Barsoum, P. Simon and Y. Gogotsi, *Nat. Energy*, 2017, **2**, 17105.
83 J. Nan, X. Guo, J. Xiao, X. Li, W. Chen, W. Wu, H. Liu, Y. Wang, M. Wu and G. Wang, *Small*, 2021, **17**, 1902085.
84 Q. Yang, Z. Huang, X. Li, Z. Liu, H. Li, G. Liang, D. Wang, Q. Huang, S. Zhang, S. Chen and C. Zhi, *ACS Nano*, 2019, **13**, 8275–8283.
85 X. Li, Y. Ma, Y. Yue, G. Li, C. Zhang, M. Cao, Y. Xiong, J. Zou, Y. Zhou and Y. Gao, *Chem. Eng. J.*, 2022, **428**, 130965.

86 K. Mao, J. Shi, Q. Zhang, Y. Hou, L. Wen, Z. Liu, F. Long, K. Niu, N. Liu, F. Long and Y. Gao, *Nano Energy*, 2022, **103**, 107791.
87 Y. Lv, L. Zhang, X. Wei, B. Qiu, W. Zhang, Q. Qin, D. Jia, X. He, Z. Liu and F. Wei, *SM&T*, 2023, **35**, e00536.
88 Z. Huang, A. Chen, F. Mo, G. Liang, X. Li, Q. Yang, Y. Guo, Z. Chen, Q. Li, B. Dong and C. Zhi, *Adv. Energy Mater.*, 2020, **10**, 2001024.
89 Z. Huang, T. Wang, H. Song, X. Li, G. Liang, D. Wang, Q. Yang, Z. Chen, L. Ma and Z. Liu, *Angew. Chem.*, 2021, **133**, 1024–1034.
90 Z. Jian, N. Yang, M. Vogel, S. Leith, A. Schulte, H. Schönherr, T. Jiao, W. Zhang, J. Müller, B. Butz and X. Jiang, *Adv. Energy Mater.*, 2020, **10**, 2002202.
91 Q. Guo, Y. Han, N. Chen and L. Qu, *ACS Energy Lett.*, 2021, **6**, 1786–1794.
92 H. Liu, X. Liu, S. Wang, H.-K. Liu and L. Li, *Energy Stor. Mater.*, 2020, **28**, 122–145.
93 M. Mustaqeem, G. A. Naikoo, M. Yarmohammadi, M. Z. Pedram, H. Pourfarzad, R. A. Dar, S. A. Taha, I. U. Hassan, M. Y. Bhat and Y.-F. Chen, *J. Energy Storage*, 2022, **55**, 105419.
94 L. Dong, W. Yang, W. Yang, C. Wang, Y. Li, C. Xu, S. Wan, F. He, F. Kang and G. Wang, *Nanomicro Lett.*, 2019, **11**, 94.
95 Q. Chen, J. Jin, Z. Kou, C. Liao, Z. Liu, L. Zhou, J. Wang and L. Mai, *Small*, 2020, **16**, 2000091.
96 D. Han, S. Wu, S. Zhang, Y. Deng, C. Cui, L. Zhang, Y. Long, H. Li, Y. Tao, Z. Weng, Q.-H. Yang and F. Kang, *Small*, 2020, **16**, 2001736.
97 G.-H. An, J. Hong, S. Pak, Y. Cho, S. Lee, B. Hou and S. Cha, *Adv. Energy Mater.*, 2020, **10**, 1902981.
98 X. Ma, J. Cheng, L. Dong, W. Liu, J. Mou, L. Zhao, J. Wang, D. Ren, J. Wu, C. Xu and F. Kang, *Energy Stor. Mater.*, 2019, **20**, 335–342.
99 H. Ren, L. Zhang, J. Zhang, T. Miao, R. Yuan, W. Chen, Z. Wang, J. Yang and B. Zhao, *Carbon*, 2022, **198**, 46–56.
100 S. Liu, L. Kang, J. M. Kim, Y. T. Chun, J. Zhang and S. C. Jun, *Adv. Energy Mater.*, 2020, **10**, 2000477.
101 G. Fang, J. Zhou, A. Pan and S. Liang, *ACS Energy Lett.*, 2018, **3**, 2480–2501.
102 X. Ma, J. Wang, X. Wang, L. Zhao and C. Xu, *J. Mater. Sci.: Mater. Electron.*, 2019, **30**, 5478–5486.
103 Q. Wang, S. Wang, J. Li, L. Ruan, N. Wei, L. Huang, Z. Dong, Q. Cheng, Y. Xiong and W. Zeng, *Adv. Electron. Mater.*, 2020, **6**, 2000388.
104 D. Guo, Z. Li, D. Wang, M. Sun and H. Wang, *ChemSusChem*, 2021, **14**, 2205–2215.
105 W. Ye, H. Wang, J. Ning, Y. Zhong and Y. Hu, *J. Energy Chem.*, 2021, **57**, 219–232.
106 S. Wu, Y. Chen, T. Jiao, J. Zhou, J. Cheng, B. Liu, S. Yang, K. Zhang and W. Zhang, *Adv. Energy Mater.*, 2019, **9**, 1902915.
107 F. Béguin, V. Presser, A. Balducci and E. Frackowiak, *Adv. Mater.*, 2014, **26**, 2219–2251.
108 H. Wang, M. Wang and Y. Tang, *Energy Stor. Mater.*, 2018, **13**, 1–7.
109 H. Zhou, C. Liu, J.-C. Wu, M. Liu, D. Zhang, H. Song, X. Zhang, H. Gao, J. Yang and D. Chen, *J. Mater. Chem. A*, 2019, **7**, 9708–9715.
110 S. Pappu, S. Anandan, T. N. Rao, S. K. Martha and S. V. Bulusu, *J. Energy Storage*, 2022, **50**, 104598.
111 S. Zhang, N. Yu, S. Zeng, S. Zhou, M. Chen, J. Di and Q. Li, *J. Mater. Chem. A*, 2018, **6**, 12237–12243.
112 H. Li, C. Han, Y. Huang, Y. Huang, M. Zhu, Z. Pei, Q. Xue, Z. Wang, Z. Liu, Z. Tang, Y. Wang, F. Kang, B. Li and C. Zhi, *Energy Environ.*, 2018, **11**, 941–951.
113 Q. Zhou, J. Ma, S. Dong, X. Li and G. Cui, *Adv. Mater.*, 2019, **31**, 1902029.
114 L. Yang, L. Song, Y. Feng, M. Cao, P. Zhang, X.-F. Zhang and J. Yao, *J. Mater. Chem. A*, 2020, **8**, 12314–12318.
115 L. Han, H. Huang, X. Fu, J. Li, Z. Yang, X. Liu, L. Pan and M. Xu, *Chem. Eng. J.*, 2020, **392**, 123733.
116 L. Han, H. Huang, J. Li, X. Zhang, Z. Yang, M. Xu and L. Pan, *J. Mater. Chem. A*, 2020, **8**, 15042–15050.
117 J. Liu, Z. Khanam, S. Ahmed, T. Wang, H. Wang and S. Song, *ACS Appl. Mater. Interfaces*, 2021, **13**, 16454–16468.
118 Q. Chen, J. Zhao, Z. Chen, Y. Jin and J. Chen, *Int. J. Hydrogen Energy*, 2022, **47**, 23909–23918.
119 C. Huang, X. Zhao, Y. Xu, Y. Zhang, Y. Yang, A. Hu, Q. Tang, X. Song, C. Jiang and X. Chen, *ACS Sustainable Chem. Eng.*, 2020, **8**, 16028–16036.
120 T. Ni, S. Wang, J. Shi, X. Du, Q. Cheng, Z. Dong, L. Ruan, W. Zeng, X. Guo, X. Ren and Z. Huang, *Adv. Mater. Technol.*, 2020, **5**, 2000268.
121 L. Li, W. Liu, K. Jiang, D. Chen, F. Qu and G. Shen, *Nanomicro Lett.*, 2021, **13**, 100.
122 Z. Cao, J. Fu, M. Wu, T. Hua and H. Hu, *Energy Stor. Mater.*, 2021, **40**, 10–21.
123 L. Wang, L. Wen, Y. Tong, S. Wang, X. Hou, X. An, S. X. Dou and J. Liang, *Carbon Energy*, 2021, **3**, 225–252.
124 Q. Zeng, Y. Lai, L. Jiang, F. Liu, X. Hao, L. Wang and M. A. Green, *Adv. Energy Mater.*, 2020, **10**, 1903930.
125 B. D. Boruah, A. Mathieson, B. Wen, C. Jo, F. Deschler and M. De Volder, *Nano Lett.*, 2020, **20**, 5967–5974.
126 B. D. Boruah, B. Wen, S. Nagane, X. Zhang, S. D. Stranks, A. Boies and M. De Volder, *ACS Energy Lett.*, 2020, **5**, 3132–3139.
127 S. Kumar, G. Saeed, L. Zhu, K. N. Hui, N. H. Kim and J. H. Lee, *Chem. Eng. J.*, 2021, **403**, 126352.
128 J. W. Gittins, C. J. Balhatchet, S. M. Fairclough and A. C. Forse, *Chem. Sci.*, 2022, **13**, 9210–9219.